

Event-Triggered Algorithms for Leader-Follower Consensus of Networked Euler-Lagrange Agents

Qingchen Liu, Mengbin Ye, Jiahu Qin and Changbin Yu

Abstract—This paper proposes three different distributed event-triggered control algorithms to achieve leader-follower consensus for a network of Euler-Lagrange agents. We firstly propose two model-independent algorithms for a subclass of Euler-Lagrange agents without the vector of gravitational potential forces. By model-independent, we mean that each agent can execute its algorithm with no knowledge of the agent self-dynamics. A variable-gain algorithm is employed when the sensing graph is undirected; algorithm parameters are selected in a fully distributed manner with much greater flexibility compared to all previous work concerning event-triggered consensus problems. When the sensing graph is directed, a constant-gain algorithm is employed. The control gains must be centrally designed to exceed several lower bounding inequalities which require limited knowledge of bounds on the matrices describing the agent dynamics, bounds on network topology information and bounds on the initial conditions. When the Euler-Lagrange agents have dynamics which include the vector of gravitational potential forces, an adaptive algorithm is proposed which requires more information about the agent dynamics but can estimate uncertain agent parameters.

For each algorithm, a trigger function is proposed to govern the event update times. At each event, the controller is updated, which ensures that the control input is piecewise constant and saves energy resources. We analyse each controllers and trigger function and exclude Zeno behaviour. Extensive simulations show 1) the advantages of our proposed trigger function as compared to those in existing literature, and 2) the effectiveness of our proposed controllers.

I. INTRODUCTION

The field of multi-agent systems has received extensive attention from the control community in the past two decades. In particular, coordination of a network of interacting agents to achieve a global objective has been seen as a key sub-area within the field. See [1] for a recent survey. Leader-follower consensus is a variation of the commonly studied consensus problem where, with all agents having a commonly defined state variable(s), the network of follower agents converge to the state values of the stationary leader. This is achieved by interaction between neighbouring agents. By the fact that interaction is only between neighbouring agents then each follower agent must use a distributed controller, i.e. agents cannot use global information about the whole network [2].

The Euler-Lagrange equations describe the dynamics of a large class of nonlinear systems (including many mechan-

ical systems such as robotic manipulators, spacecraft and marine vessels) [3], [4]. As a result, there is motivation to study multi-agent coordination problems where each agent has Euler-Lagrange dynamics [5]. Leader-follower consensus for directed networks of Euler-Lagrange agents has been studied in [6] using a model-independent controller, and in [7] using an adaptive controller. In both, the topology requires a directed spanning tree.

Recently, use of event-triggered controllers has been popularised in multi-agent coordination problems [8]. While each agent has continuous time dynamics, the controller is updated at discrete time instants based on event-scheduling. Because the controller updates occur at specific events, this has the benefit of reducing actuator updates. However, it is important to properly design and analyse the event-scheduling trigger function to exclude Zeno behaviour [9], [10], which can cause the controller to collapse. Numerous results have been published studying consensus based problems using distributed event-triggered control laws. However, the majority study agents with single and double-integrator dynamics [11]–[16].

There have been relatively few results published studying event-triggered control for networks of Euler-Lagrange agents. Pioneering contributions studied leaderless consensus (but not leader-follower consensus) on an undirected network [17], [18]. The dynamics studied in [17] and [18] are a subclass of Euler-Lagrange dynamics as they do not consider the presence of gravitational forces for each agent. While continuous model-independent algorithms e.g. [6] are easily adapted to be event-triggered, as shown in [17], [18], they cannot guarantee the coordination objective in the presence of gravitational forces (which has an effect which is similar to a bounded disturbance). Typical control techniques required to deal with this term include feedback linearisation [19], adaptive control [7] and sliding mode control [20]. We note that these techniques have not been well studied in an event-triggered framework. In fact, first-order sliding mode controllers exhibit Zeno-like behaviour and thus are unsuitable for implementation in event-triggered control. In [21], an adaptive, event-triggered controller is proposed to achieve flocking behaviour for undirected networks of Euler-Lagrange agents. This allows for gravitational forces omitted in [17], [18]. However, the proposed controller is piecewise continuous, which restricts its implementation in digital platforms. Moreover, it is worth noting that the trigger function used in [21] cannot eliminate Zeno behaviour for each agent.

Q. Liu, M. Ye and C. Yu are with the Research School of Engineering, Australian National University, Canberra ACT 0200, Australia. C. Yu is also with the School of Automation, Hangzhou Dianzi University, Hangzhou 310018, China. {qingchen.liu, mengbin.ye, brad.yu}@anu.edu.au.

J. Qin is with the Department of Automation, University of Science and Technology of China, Hefei 230027, China. jhqin@ustc.edu.cn

A. Contributions of This Paper

In this paper, we propose three different distributed event-triggered control algorithms to achieve leader-follower consensus for networked Euler-Lagrange agents; each algorithm has different strengths and their appropriateness of use may depend on the application scenario.

We propose two model-independent controllers for Euler-Lagrange agents without the gravitational term (unlike the model-dependent algorithm in [17]). Firstly, a globally asymptotically stable variable-gain model-independent algorithm is proposed for agents on undirected graphs. The variable-gain controller allows for fully distributed and *arbitrary design of parameters* in both the control algorithm and trigger function. *For agents with complex dynamics, almost all existing results require centralised design of key parameters in the trigger function using limited global knowledge of the network [17], [21], [22]. The design of these key parameters is to ensure either Zeno-free behaviour, or to guarantee convergence of the controller. In the case of simple agent dynamics, the parameters are distributed in design but must either obey upper or lower bounds [11]–[13], [23].* As such, the fully distributed variable-gain controller represents a significant advance on existing event-triggered control algorithms, because stability and convergence are always guaranteed, even if the algorithm and trigger function parameters are arbitrarily selected.

Even when implemented continuously, and with simple agent dynamics, variable-gain algorithms on directed graphs are difficult to analyse [24]–[26]. For the second model-independent controller, which is applicable for directed graphs, we are therefore motivated to use constant control gains. It will become apparent in the sequel that, even when the controller has constant gains, the combination of Euler-Lagrange dynamics, directed topology, and event-based control requires non-trivial stability analysis. The algorithm achieves leader-follower consensus semi-globally, exponentially fast (neither directed graphs nor exponential stability has not been established in any existing results on event-based networks of Euler-Lagrange agents). Some limited knowledge of the bounds on the agent dynamic parameters, the network topology and a set of all possible initial conditions is required to centrally design the control gains. This is a trade-off for allowing agents to interact on a directed graph.

Lastly, we propose a globally asymptotically stable adaptive algorithm for use when the gravitational term is present in the agent self-dynamics; this algorithm appeared in our preliminary work [27]. The adaptive algorithm is able to estimate uncertain dynamical parameters, but requires increased knowledge about the agent self-dynamics.

All three proposed controllers are piecewise constant (unlike the piecewise continuous algorithm in [21]), which has the benefit of reducing actuator updates and thus conserving energy resources. Furthermore, each agent only requires state, and relative state measurements, and does not require knowledge of the trigger times of neighbouring agents (unlike [17], [21]). For each algorithm, a trigger function is proposed and we show that Zeno behaviour can be excluded for every agent by proving that for any finite interval of time, a strictly

positive lower bound exists on the time between each event. All three trigger functions are of the same form with only minor modifications. Each term of the trigger function is carefully selected to ensure that the trigger function is more effective, when compared with existing trigger functions which do one or the other, at 1) reducing the total number of events, and 2) eliminating Zeno behaviour for every agent. We show this by detailed comparison and analysis based on simulations. As a result of having multiple terms in the trigger function to achieve the aforementioned improvements, the stability analysis is made significantly more complicated. Each algorithm requires a different approach to proving stability, and the proposed methods may be useful for other problems in event-based control of multi-agent systems.

B. Structure of the Rest of the Paper

Section II provides mathematical notations and background on graph theory and Euler-Lagrange systems. A formal problem definition is also provided. The three different distributed event-triggered control algorithms are then proposed and analysed in Section III, IV and V, separately. Simulations in Section VI show the effectiveness of the proposed controllers. Concluding remarks are given in Section VII.

II. BACKGROUND AND PROBLEM STATEMENT

A. Notations and Mathematical Preliminaries

In this paper, \mathbb{R}^n denotes the n -dimensional Euclidean space and $\mathbb{R}^{m \times n}$ denotes the set of $m \times n$ real matrices. The transpose of a vector or matrix \mathbf{A} is given by \mathbf{A}^\top . The i^{th} smallest eigenvalue of a symmetric matrix \mathbf{A} is denoted by $\lambda_i(\mathbf{A})$. Let $\mathbf{x} = [\mathbf{x}_1, \dots, \mathbf{x}_n]^\top$ where $\mathbf{x}_i \in \mathbb{R}^{n \times n}$ and $n \geq 1$. Then $\text{diag}\{\mathbf{x}\}$ denotes a (block) diagonal matrix with the (block) elements of \mathbf{x} on its diagonal, i.e. $\text{diag}\{\mathbf{x}_1, \dots, \mathbf{x}_n\}$. A symmetric matrix $\mathbf{A} \in \mathbb{R}^{n \times n}$ which is positive definite (respectively nonnegative definite) is denoted by $\mathbf{A} > 0$ (respectively $\mathbf{A} \geq 0$). For two symmetric matrices \mathbf{A}, \mathbf{B} , the expression $\mathbf{A} > \mathbf{B}$ is equivalent to $\mathbf{A} - \mathbf{B} > 0$. The $n \times n$ identity matrix is \mathbf{I}_n and $\mathbf{1}_n$ denotes an n -tuple column vector of all ones. The $n \times 1$ column vector of all zeros is denoted by $\mathbf{0}_n$. The symbol \otimes denotes the Kronecker product. The Euclidean norm of a vector, and the matrix norm induced by the Euclidean norm, are denoted by $\|\cdot\|$. The absolute value of a real number is $|\cdot|$. For the space of piecewise continuous, bounded vector functions, the norm is defined as $\|f\|_{\mathcal{L}_\infty} = \sup \|f(t)\| < \infty$ and the space is denoted by \mathcal{L}_∞ . The space \mathcal{L}_p for $1 \leq p < \infty$ is defined as the set of all piecewise continuous vector functions such that $\|f\|_{\mathcal{L}_p} = (\int_0^\infty \|f(t)\|^p dt)^{1/p} < \infty$ where p refers to the type of p -norm.

Several theorems, lemmas and corollaries are now introduced, which will be used in this paper.

Theorem 1 (Mean Value Theorem for Vector-Valued Functions [28]). *For a continuous vector-valued function $\mathbf{f}(s) : \mathbb{R} \rightarrow \mathbb{R}^n$ differentiable on $s \in [a, b]$, there exists $t \in (a, b)$ such that*

$$\left\| \frac{d\mathbf{f}}{ds}(t) \right\| \geq \frac{1}{b-a} \|\mathbf{f}(b) - \mathbf{f}(a)\|$$

Theorem 2 (The Schur Complement [29]). *Consider a symmetric block matrix, partitioned as*

$$\mathbf{A} = \begin{bmatrix} \mathbf{B} & \mathbf{C} \\ \mathbf{C}^\top & \mathbf{D} \end{bmatrix} \quad (1)$$

Then $\mathbf{A} > 0$ if and only if $\mathbf{B} > 0$ and $\mathbf{D} - \mathbf{C}^\top \mathbf{B}^{-1} \mathbf{C} > 0$. Equivalently, $\mathbf{A} > 0$ if and only if $\mathbf{D} > 0$ and $\mathbf{B} - \mathbf{C} \mathbf{D}^{-1} \mathbf{C}^\top > 0$.

Lemma 1. (From [30]) *If a function $f(t)$ satisfies $f(t), \dot{f}(t) \in L_\infty$, and $f(t) \in L_p$ for some value of $p \in [1, \infty)$, then $f(t) \rightarrow 0$ as $t \rightarrow \infty$.*

Lemma 2. *Suppose $\mathbf{A} > 0$ is defined as in (1). Let a quadratic function with arguments \mathbf{x}, \mathbf{y} be expressed as $W = [\mathbf{x}^\top, \mathbf{y}^\top] \mathbf{A} [\mathbf{x}^\top, \mathbf{y}^\top]^\top$. Define $\mathbf{F} := \mathbf{B} - \mathbf{C} \mathbf{D}^{-1} \mathbf{C}^\top$ and $\mathbf{G} := \mathbf{D} - \mathbf{C}^\top \mathbf{B}^{-1} \mathbf{C}$. Then there holds*

$$\lambda_{\min}(\mathbf{F}) \mathbf{x}^\top \mathbf{x} \leq \mathbf{x}^\top \mathbf{F} \mathbf{x} \leq W \quad (2a)$$

$$\lambda_{\min}(\mathbf{G}) \mathbf{y}^\top \mathbf{y} \leq \mathbf{y}^\top \mathbf{G} \mathbf{y} \leq W \quad (2b)$$

Proof. The proof for (2b) is immediately obtained by recalling **Theorem 2** and observing that

$$W = \mathbf{y}^\top \mathbf{G} \mathbf{y} + [\mathbf{y}^\top \mathbf{C}^\top \mathbf{B}^{-1} + \mathbf{x}^\top] \mathbf{B} [\mathbf{B}^{-1} \mathbf{C} \mathbf{y} + \mathbf{x}]$$

An equally straightforward proof yields (2a). \square

Lemma 3. *Let $g(x, y)$ be a function given as*

$$g(x, y) = ax^2 + by^2 - cxy^2 - dxy \quad (3)$$

for real positive scalars $a, c, d > 0$. Then for a given $\mathcal{X} > 0$, there exist $b > 0$ such that $g(x, y) > 0$ for all $y \in [0, \infty)$ and $x \in [0, \mathcal{X}]$.

Proof. See Appendix A. \square

Corollary 1. *Let $h(x, y)$ be a function given as*

$$h(x, y) = ax^2 + by^2 - cxy^2 - dxy - ex - fy \quad (4)$$

where the real, strictly positive scalars c, d, e, f and two further positive scalars ε, ϑ are fixed. Suppose that for given \mathcal{Y}, ε there holds $\mathcal{Y} - \varepsilon > 0$, and for a given $\mathcal{X} > 0$ there holds $\mathcal{X} - \vartheta > 0$. Define the sets $\mathcal{U} = \{x, y : x \in [\mathcal{X} - \vartheta, \mathcal{X}], y > 0\}$ and $\mathcal{V} = \{x, y : x > 0, y \in [\mathcal{Y} - \varepsilon, \mathcal{Y}]\}$. Define the region $\mathcal{R} = \mathcal{U} \cup \mathcal{V}$. Then there exist $a, b > 0$ such that $h(x, y)$ is positive definite in \mathcal{R} .

Proof. See Appendix A. \square

B. Graph Theory

We model the interactions among the leader and n followers by a weighted directed graph (digraph) $\mathcal{G} = (\mathcal{V}, \mathcal{E}, \mathcal{A})$ with vertex set $\mathcal{V} = \{v_0, v_1, \dots, v_n\}$ and edge set $\mathcal{E} \subseteq \mathcal{V} \times \mathcal{V}$. Without loss of generality, the leader agent is numbered by v_0 . We use \mathcal{G}_F to describe the interactions among the n follower agents with vertex set $\mathcal{V}_F = \{v_1, \dots, v_n\}$ and edge set $\mathcal{E}_F \subseteq \mathcal{V}_F \times \mathcal{V}_F$. An ordered edge set of \mathcal{G} is $e_{ij} = (v_i, v_j)$. The weighted adjacency matrix $\mathcal{A} = \mathcal{A}(\mathcal{G}) = \{a_{ij}\}$ is the $(n+1) \times (n+1)$ matrix given by $a_{ij} > 0$, if $e_{ji} \in \mathcal{E}$ and $a_{ij} = 0$, otherwise. In this paper, it is assumed that $a_{ii} = 0$, i.e. there

are no self-loops. The edge e_{ij} is incoming with respect to v_j and outgoing with respect to v_i . A graph is undirected if $e_{ij} \in \mathcal{E} \Leftrightarrow e_{ji} \in \mathcal{E}$ and $a_{ij} = a_{ji}$. The neighbour set of v_i is denoted by $\mathcal{N}_i = \{v_j \in \mathcal{V} : (v_i, v_j) \in \mathcal{E}\}$. The $(n+1) \times (n+1)$ Laplacian matrix, $\mathcal{L} = \{l_{ij}\}$, of the associated directed graph \mathcal{G} is defined as

$$l_{ij} = \begin{cases} \sum_{k=1, k \neq i}^n a_{ik} & \text{for } j = i \\ -a_{ij} & \text{for } j \neq i \end{cases}$$

A digraph with $n+1$ vertices is called a directed spanning tree if it has n edges and there exists a root vertex with directed paths to every other vertex [2]. The following result holds for the Laplacian matrix associated with a directed graph.

Lemma 4. (From [2]) *Let \mathcal{L} be the Laplacian matrix associated with a directed graph. Then \mathcal{L} has a simple zero eigenvalue and all other eigenvalues have positive real parts if and only if \mathcal{G} has a directed spanning tree.*

Lemma 5. (From [31]) *Suppose a graph \mathcal{G} contains a directed spanning tree, and there are no edges of \mathcal{G} which are incoming to the root vertex v_0 of the tree. Then the Laplacian matrix associated with \mathcal{G} has the following form:*

$$\mathcal{L} = \begin{bmatrix} 0 & \mathbf{0}_{n-1}^\top \\ \mathcal{L}_{21} & \mathcal{L}_{22} \end{bmatrix}$$

and all eigenvalues of \mathcal{L}_{22} have positive real parts. Moreover, there exists a diagonal positive definite matrix $\mathbf{\Gamma}$ such that $\mathbf{Q} := \mathbf{\Gamma} \mathcal{L}_{22} + \mathcal{L}_{22}^\top \mathbf{\Gamma} > 0$. In addition, if \mathcal{G}_F is undirected, then \mathcal{L}_{22} is symmetric positive definite.

C. Euler-Lagrange Systems

A class of dynamical systems can be described using the Euler-Lagrange equations [3]. The general form for the i^{th} agent equation of motion is:

$$\mathbf{M}_i(\mathbf{q}_i) \ddot{\mathbf{q}}_i + \mathbf{C}_i(\mathbf{q}_i, \dot{\mathbf{q}}_i) \dot{\mathbf{q}}_i + \mathbf{g}_i(\mathbf{q}_i) = \boldsymbol{\tau}_i \quad (5)$$

where $\mathbf{q}_i \in \mathbb{R}^p$ is a vector of the generalized coordinates, $\mathbf{M}_i(\mathbf{q}_i) \in \mathbb{R}^{p \times p}$ is the inertial matrix, $\mathbf{C}_i(\mathbf{q}_i, \dot{\mathbf{q}}_i) \in \mathbb{R}^{p \times p}$ is the Coriolis and centrifugal torque matrix, $\mathbf{g}_i(\mathbf{q}_i) \in \mathbb{R}^p$ is the vector of gravitational forces and $\boldsymbol{\tau}_i \in \mathbb{R}^p$ is the control input vector. For agent i , we have $\mathbf{q}_i = [\mathbf{q}_i^{(1)}, \dots, \mathbf{q}_i^{(p)}]^\top$. We assume each agent is fully actuated. The dynamics in (5) are assumed to satisfy the following properties, details of which are provided in [3].

- P1 The matrix $\mathbf{M}_i(\mathbf{q}_i)$ is symmetric positive definite.
- P2 There exist constants $k_{\underline{m}}, k_{\overline{m}} > 0$ such that $k_{\underline{m}} \mathbf{I}_p \leq \mathbf{M}_i(\mathbf{q}_i) \leq k_{\overline{m}} \mathbf{I}_p, \forall i, \mathbf{q}_i$. It follows that $\sup_{\mathbf{q}_i} \|\mathbf{M}_i\|_2 \leq k_{\overline{m}}$ and $k_{\underline{m}} \leq \inf_{\mathbf{q}_i} \|\mathbf{M}_i^{-1}\|_2^{-1} \forall i$.
- P3 There exists a constant $k_C > 0$ such that $\|\mathbf{C}_i\|_2 \leq k_C \|\dot{\mathbf{q}}_i\|_2, \forall i, \dot{\mathbf{q}}_i$.
- P4 The matrix $\mathbf{C}_i(\mathbf{q}_i, \dot{\mathbf{q}}_i)$ is related to the inertial matrix $\mathbf{M}_i(\mathbf{q}_i, \dot{\mathbf{q}}_i)$ by the expression $\mathbf{x}^\top (\frac{1}{2} \dot{\mathbf{M}}_i(\mathbf{q}_i) - \mathbf{C}_i(\mathbf{q}_i, \dot{\mathbf{q}}_i)) \mathbf{x} = 0$ for any $\mathbf{q}, \dot{\mathbf{q}}, \mathbf{x} \in \mathbb{R}^p$. This implies that $\mathbf{M}_i(\mathbf{q}_i) = \mathbf{C}_i(\mathbf{q}_i, \dot{\mathbf{q}}_i) + \mathbf{C}_i(\mathbf{q}_i, \dot{\mathbf{q}}_i)^\top$.
- P5 There exists a constant $k_g > 0$ such that $\|\mathbf{g}_i(\mathbf{q}_i)\| < k_g$.
- P6 Linearity in the parameters: $\mathbf{M}_i(\mathbf{q}_i) \mathbf{x} + \mathbf{C}_i(\mathbf{q}_i, \dot{\mathbf{q}}_i) \mathbf{y} + \mathbf{g}_i(\mathbf{q}_i) = \mathbf{Y}_i(\mathbf{q}_i, \dot{\mathbf{q}}_i, \mathbf{x}, \mathbf{y}) \boldsymbol{\Theta}_i$ for all vectors $\mathbf{x}, \mathbf{y} \in \mathbb{R}^p$,

where $Y_i(\mathbf{q}_i, \dot{\mathbf{q}}_i, \mathbf{x}, \mathbf{y})$ is the known regressor matrix and Θ_i is a vector of unknown but constant parameters associated with the i^{th} agent.

Remark 1. *It is assumed throughout this paper that the properties P1 through to P6 always hold.*

Assumption 1 (Sub-class of dynamics). *In Sections III and IV, we assume that $\mathbf{g}_i(\mathbf{q}_i) = \mathbf{0}, \forall i$. In other words, the dynamics of the agents belong to a subclass of Euler-Lagrange equations which do not have a gravity term. That is,*

$$M_i(\mathbf{q}_i)\ddot{\mathbf{q}}_i + C_i(\mathbf{q}_i, \dot{\mathbf{q}}_i)\dot{\mathbf{q}}_i = \boldsymbol{\tau}_i \quad (6)$$

If the gravity term $\mathbf{g}_i(\mathbf{q}_i)$ is present, the adaptive controller proposed in Section V may be used.

D. Problem Statement

Denote the leader as agent 0 with \mathbf{q}_0 and $\dot{\mathbf{q}}_0$ being the generalised coordinates and generalised velocity of the leader, respectively. The aim is to develop event-based, distributed algorithms for each Euler-Lagrange follower agent, where the updates are such that τ_i is piecewise-constant. The distributed algorithms are designed to achieve leader-follower consensus to a stationary leader, i.e. $\dot{\mathbf{q}}_0(t) = 0, \forall t \geq 0$. Leader-follower consensus is said to be achieved if $\lim_{t \rightarrow \infty} \|\mathbf{q}_i(t) - \mathbf{q}_0(t)\| = 0, \forall i = 1, \dots, n$ and $\lim_{t \rightarrow \infty} \|\dot{\mathbf{q}}_i(t)\| = 0, \forall i = 1, \dots, n$ are satisfied.

Another aim of this paper is to exclude the possibility of Zeno behaviour. We provide a formal definition of Zeno behaviour in the sequel. Zeno behaviour of an event-based controller means an infinite number of controller updates occur in a finite time period, which is undesirable since no practical controller can do this.

In this paper, we assume that agent $i \in 1, \dots, n$ is equipped with sensors which continuously measures the relative generalised coordinates to agent i 's neighbours. In other words, $\mathbf{q}_i(t) - \mathbf{q}_j(t), \forall j \in \mathcal{N}_i$ is available to agent i . In Section IV we also assume that the relative generalised velocities are available, i.e. $\dot{\mathbf{q}}_i(t) - \dot{\mathbf{q}}_j(t), \forall j \in \mathcal{N}_i$. The scenario where agents collect relative information to execute algorithms can be found in many experimental testbeds, such as ground robots or UAVs equipped with high-speed cameras. It is also assumed that each agent i can measure its own generalised velocity continuously, $\dot{\mathbf{q}}_i(t)$.

Definition 1. *Let a finite time interval be $t_Z = [a, b]$ where $0 \leq a < b < \infty$. If, for some finite $k \geq 0$, the sequence of event triggers $\{t_k^i, \dots, t_\infty^i\} \in [a, b]$ then the system exhibits Zeno behaviour.*

III. MAIN RESULT: A VARIABLE-GAIN, MODEL-INDEPENDENT CONTROLLER ON UNDIRECTED NETWORKS

In this section, we introduce a variable gain, event-triggered control algorithm to achieve leader-follower consensus for Euler-lagrange agents where the network model of the follower agents is described by an undirected network. We show that the proposed algorithm do not require any knowledge of the multi-agent system (i.e totally distributed design) and is globally

stable. Zeno behaviour is also excluded for each agent in the system.

A. Main Result

Define a new state variable for agent i as

$$\mathbf{z}_i(t) = \sum_{j=0}^n a_{ij}(\mathbf{q}_i(t) - \mathbf{q}_j(t)) + \mu_i(t)\dot{\mathbf{q}}_i(t), \quad i = 1, \dots, n$$

where a_{ij} is an element of the adjacency matrix \mathcal{A} associated with the digraph \mathcal{G} . Note that the follower graph \mathcal{G}_F is undirected. We let $\mu_i(t)$ be subject to the following updating law:

$$\dot{\mu}_i(t) = \alpha \dot{\mathbf{q}}_i^\top(t) \dot{\mathbf{q}}_i(t) \quad (7)$$

The scalar α is strictly positive and is universal for all agents. It is obvious that $\mu_i(t)$ is a monotonically increasing function. The variable-gain scalar function $\mu_i(t)$ is initialised at $t = 0$ with an arbitrary $\mu_i(0) \geq 0$, which implies that $\mu_i(t) \geq 0, \forall t > 0$.

The control algorithm is now proposed. Let the trigger time sequence of agent i be $t_0^i, t_1^i, \dots, t_k^i, \dots$ with $t_0^i := 0$ and we detail below how each trigger time is determined. The event-triggered controller for follower agent i is designed as:

$$\boldsymbol{\tau}_i(t) = -\mathbf{z}_i(t_k^i) \quad (8)$$

for $t \in [t_k^i, t_{k+1}^i)$. The control input for each agent is held constant and equal to the last control update $\boldsymbol{\tau}_i(t_k^i)$ in the time interval $[t_k^i, t_{k+1}^i)$.

We define a state mismatch for agent i between consecutive event times t_k^i and t_{k+1}^i as follows:

$$\mathbf{e}_i(t) = \mathbf{z}_i(t_k^i) - \mathbf{z}_i(t) \quad (9)$$

for $t \in [t_k^i, t_{k+1}^i)$. Then we design the trigger function as follows:

$$f_i(\mathbf{e}_i, \dot{\mathbf{q}}_i, \omega_i) = \|\mathbf{e}_i(t)\|^2 - \beta_i \|\dot{\mathbf{q}}_i(t)\|^2 - \omega_i(t) \quad (10)$$

where β_i is an arbitrarily chosen positive constant (see the Proof of **Theorem 3** for the explanations), $\omega_i(t)$ is an offset function defined as $\omega_i(t) = \kappa_i \exp(-\varepsilon_i t)$ with arbitrarily chosen $\kappa_i, \varepsilon_i > 0$. The k^{th} event for agent i is triggered as soon as the trigger condition $f_i(\mathbf{e}_i, \dot{\mathbf{q}}_i, \omega_i) = 0$ is satisfied. The control input $\boldsymbol{\tau}_i(t)$ is updated only when an event of agent i is triggered. Furthermore, every time an event is triggered, and in accordance with their definitions, the measurement error $\mathbf{e}_i(t)$ is reset to be equal to zero and thus the trigger function assumes a non-positive value, that is, $f_i(\mathbf{e}_i, \dot{\mathbf{q}}_i, \omega_i) \leq 0$.

Remark 2. *In existing event-based multi-agent control literature, the parameters of the state-dependent term are typically restricted. For example, the authors of [18] studied an event-triggered controller which achieved leaderless consensus for networked Euler-Lagrange agents under an undirected graph. Different from our proposed variable-gain controller, their controller adopts fixed gains. As a result, the parameter ϱ_i (see the trigger function in [18]) of the state-dependent term has to be less than a computable upper bound. This bound requires knowledge of the control gains and graph topology (e.g.*

number of neighbours and degree of the agent). In comparison, our equivalent parameter β_i in our proposed trigger function (10) can be chosen as an arbitrary positive constant. This provides a much greater flexibility in the implementation of the algorithm.

We note that even in papers considering simple single integrator dynamics with a parameter for the state-dependent term, equivalent to our β_i , require an upper bound as well (see the seminal works of [11], [13]). To the best of the authors' knowledge, the event-based controller proposed in this paper is the first one to allow an arbitrarily chosen positive parameter for the state-dependent term in the trigger function.

By substituting the control input (8) into the system dynamics (6), the closed-loop system can be written as

$$\mathbf{M}_i(\mathbf{q}_i)\ddot{\mathbf{q}}_i(t) + \mathbf{C}_i(\mathbf{q}_i, \dot{\mathbf{q}}_i)\dot{\mathbf{q}}_i(t) = -\mathbf{z}_i(t_k^i) \quad (11)$$

Then by applying (9), we obtain

$$\mathbf{M}_i(\mathbf{q}_i)\ddot{\mathbf{q}}_i(t) + \mathbf{C}_i(\mathbf{q}_i, \dot{\mathbf{q}}_i)\dot{\mathbf{q}}_i(t) = -(\mathbf{z}_i(t) + \mathbf{e}_i(t)) \quad (12)$$

Define new state variables $\mathbf{u}_i = \mathbf{q}_i - \mathbf{q}_0$ and $\mathbf{v}_i = \dot{\mathbf{q}}_i$ and we drop the argument t for brevity, and where there is no confusion. Define the stacked column vectors of all $\mathbf{u}_i, \mathbf{v}_i, \mathbf{q}_i, \mathbf{e}_i$ as $\mathbf{u} = [\mathbf{u}_1^\top, \dots, \mathbf{u}_n^\top]^\top$, $\mathbf{v} = [\mathbf{v}_1^\top, \dots, \mathbf{v}_n^\top]^\top$, $\mathbf{q} = [\mathbf{q}_1^\top, \dots, \mathbf{q}_n^\top]^\top$, $\mathbf{z} = [\mathbf{z}_1^\top, \dots, \mathbf{z}_n^\top]^\top$ and $\mathbf{e} = [\mathbf{e}_1^\top, \dots, \mathbf{e}_n^\top]^\top$ respectively. It is easy to obtain that

$$\begin{aligned} \mathbf{z} &= (\mathbf{L}_{22} \otimes \mathbf{I}_p)(\mathbf{q} - \mathbf{1}_n \otimes \mathbf{q}_0) + \mathbf{K}\dot{\mathbf{q}} \\ &= (\mathbf{L}_{22} \otimes \mathbf{I}_p)\mathbf{u} + \mathbf{K}\mathbf{v} \end{aligned}$$

where $\mathbf{K} = \text{diag}[\mu_1 \mathbf{I}_p, \dots, \mu_n \mathbf{I}_p]$. Define the following block diagonal matrices $\mathbf{M}(\mathbf{q}) = \text{diag}[\mathbf{M}_1(\mathbf{q}_1), \dots, \mathbf{M}_n(\mathbf{q}_n)]$, $\mathbf{C}(\mathbf{q}, \dot{\mathbf{q}}) = \text{diag}[\mathbf{C}_1(\mathbf{q}_1, \dot{\mathbf{q}}_1), \dots, \mathbf{C}_n(\mathbf{q}_n, \dot{\mathbf{q}}_n)]$. It is obvious that \mathbf{M} is symmetric positive definite since $M_i > 0, \forall i$. With these notations, the compact form of system (12) can be expressed as

$$\begin{aligned} \dot{\mathbf{u}} &= \mathbf{v} \\ \dot{\mathbf{v}} &= -\mathbf{M}(\mathbf{q})^{-1} [\mathbf{C}(\mathbf{q}, \mathbf{v})\mathbf{v} + (\mathbf{L}_{22} \otimes \mathbf{I}_p)\mathbf{u} + \mathbf{K}\mathbf{v} + \mathbf{e}] \\ \dot{\mathbf{K}} &= \alpha(\mathbf{\Xi} \otimes \mathbf{I}_p) \end{aligned} \quad (13)$$

where $\mathbf{\Xi} = \text{diag}[\|\mathbf{v}_1\|_2^2, \|\mathbf{v}_2\|_2^2, \dots, \|\mathbf{v}_n\|_2^2]$. The leader-follower objective is achieved when there holds $\mathbf{u} = \mathbf{v} = \mathbf{0}_{np}$.

We now present the main result for this Section.

Theorem 3. *Suppose that each follower agent with dynamics (6), under Assumption 1, employs the controller (8) with trigger function (10). Suppose further that the directed graph \mathcal{G} contains a directed spanning tree, with the leader agent 0 as the root node (thus with no incoming edges) and the follower graph \mathcal{G}_F is undirected. Then the leader-follower consensus objective is globally asymptotically achieved and no agent will exhibit Zeno behaviour.*

Proof. We divide our proof into two parts. In the first part, we focus on the stability analysis of the system (13). Notice that (13) is non-autonomous in the sense that it is not self-contained ($\mathbf{M}_i, \mathbf{C}_i$ depend on \mathbf{q}_i and $\mathbf{q}_i, \dot{\mathbf{q}}_i$ respectively). However, study of a Lyapunov-like function shows leader-follower consensus is achieved. In the second part, analysis

is provided to show the exclusion of Zeno behaviour for each agent.

1) *Stability analysis:* Consider the following Lyapunov-like function

$$\begin{aligned} V &= \frac{1}{2} \mathbf{u}^\top (\mathbf{L}_{22} \otimes \mathbf{I}_p) \mathbf{u} + \frac{1}{2} \mathbf{v}^\top \mathbf{M} \mathbf{v} + \sum_{i=1}^n \frac{1}{2\alpha} (\mu_i - \bar{\mu})^2 \\ &= V_1 + V_2 + V_3 \end{aligned} \quad (14)$$

where $\bar{\mu}$ is a strictly positive constant. The chosen of $\bar{\mu}$ will be presented below. Since \mathcal{G} contains a directed spanning tree and \mathcal{G}_F is undirected, according to Lemma 5, \mathbf{L}_{22} is positive definite. Note that \mathbf{M} is positive definite and V_3 is non-negative, we conclude that V is strictly positive for nonzero \mathbf{u} and \mathbf{v} .

Taking the derivative of V with respect to time, along the trajectory of system (13), there holds $\dot{V} = \dot{V}_1 + \dot{V}_2 + \dot{V}_3$. Evaluating \dot{V}_1 yields

$$\dot{V}_1 = \mathbf{u}^\top (\mathbf{L}_{22} \otimes \mathbf{I}_p) \mathbf{v}$$

Next, the derivative \dot{V}_2 is evaluated to be

$$\begin{aligned} \dot{V}_2 &= \mathbf{v}^\top \mathbf{M} \dot{\mathbf{v}} + \frac{1}{2} \mathbf{v}^\top \dot{\mathbf{M}} \mathbf{v} \\ &= -\mathbf{v}^\top \mathbf{C} \mathbf{v} - \mathbf{v}^\top (\mathbf{L}_{22} \otimes \mathbf{I}_p) \mathbf{u} - \mathbf{v}^\top \mathbf{K} \mathbf{v} - \mathbf{v}^\top \mathbf{e} + \frac{1}{2} \mathbf{v}^\top \dot{\mathbf{M}} \mathbf{v} \\ &= -\mathbf{v}^\top (\mathbf{L}_{22} \otimes \mathbf{I}_p) \mathbf{u} - \mathbf{v}^\top \mathbf{K} \mathbf{v} - \mathbf{v}^\top \mathbf{e} \end{aligned}$$

Lastly, \dot{V}_3 evaluates to

$$\dot{V}_3 = \sum_{i=1}^n (\mu_i - \bar{\mu}) \mathbf{v}_i^\top \mathbf{v}_i = \mathbf{v}^\top \mathbf{K} \mathbf{v} - \bar{\mu} \mathbf{v}^\top \mathbf{v}$$

Since \mathbf{L}_{22} is symmetric, summing \dot{V}_1, \dot{V}_2 and \dot{V}_3 yields

$$\dot{V} = -\bar{\mu} \mathbf{v}^\top \mathbf{v} + \mathbf{v}^\top \mathbf{e} \quad (15)$$

By using the inequality $\mathbf{v}^\top \mathbf{e} \leq \frac{a}{2} \|\mathbf{v}\|^2 + \frac{1}{2a} \|\mathbf{e}\|^2, \forall a > 0$, we obtain

$$\dot{V} \leq \left(\frac{a}{2} - \bar{\mu}\right) \|\mathbf{v}\|^2 + \frac{1}{2a} \|\mathbf{e}\|^2$$

Note that the nonpositivity of $f_i(\mathbf{e}_i, \mathbf{v}_i, \omega_i)$ guarantees that $\|\mathbf{e}\|^2 \leq \beta \|\mathbf{v}\|^2 + \bar{\omega}(t)$, where $\beta = \max_i \{\beta_i\}$ and $\bar{\omega}(t) = \sum_{i=1}^N \omega_i(t)$. It follows that \dot{V} satisfies

$$\dot{V} \leq \left(\frac{a}{2} + \frac{\beta}{2a} - \bar{\mu}\right) \|\mathbf{v}\|^2 + \bar{\omega}(t)$$

For notation simplicity, we define $\chi = \bar{\mu} - \frac{a}{2} - \frac{\beta}{2a}$. Note that for any given a and β , we can find a sufficiently large $\bar{\mu}$ to ensure $\chi > 0$ and thus

$$\dot{V} \leq -\chi \|\mathbf{v}\|^2 + \bar{\omega}(t)$$

and it is straightforward to conclude that the parameter β_i in the trigger function (10) can be selected as an arbitrarily positive constant. Integrating both sides of the above equation from 0 to t , for any $t > 0$, yields

$$V(t) + \chi \int_0^t \|\mathbf{v}(\epsilon)\|^2 d\epsilon \leq V(0) + \sum_{i=1}^n \frac{\kappa_i}{\epsilon_i}$$

which implies that $V(t)$ and $\chi \int_0^t \|\mathbf{v}(\epsilon)\|^2 d\epsilon$ are bounded since $V(0), \kappa_i, \varepsilon_i$ are all bounded. By recalling (14), it is straightforward to conclude that $\mathbf{u}, \mathbf{v}, \mu_i$ are all bounded. Now we turn to $\dot{\mathbf{v}}_i$. Notice that $\dot{\mathbf{q}}_0 = 0$ and (11), we have

$$\dot{\mathbf{v}}_i = -\mathbf{M}_i(\mathbf{q}_i)^{-1}[\mathbf{C}_i(\mathbf{q}_i, \dot{\mathbf{q}}_i)\dot{\mathbf{q}}_i + \mathbf{z}_i(t_k^i)] \quad (16)$$

Since $\mathbf{u}, \mathbf{v}, \mu_i$ are bounded, $\dot{\mathbf{q}}_i$ and $\mathbf{z}_i(t_k^i)$ are bounded. Then by recalling properties P2 and P3, we conclude that $\dot{\mathbf{v}}$ is bounded. From the fact that both \mathbf{v} and $\dot{\mathbf{v}}$ are bounded, we obtain $\mathbf{v}, \dot{\mathbf{v}} \in \mathcal{L}_\infty$. Moreover, the boundedness of $\chi \int_0^t \|\mathbf{v}(\epsilon)\|^2 d\epsilon$ indicates $\mathbf{v} \in \mathcal{L}_2$. By applying **Lemma 1**, we conclude that $\mathbf{v} \rightarrow \mathbf{0}_{np}$ as $t \rightarrow \infty$. From (7) we observe that μ_i is strictly monotonically increasing. Combining this with the fact that $\mu_i \geq 0$ is bounded, we conclude that $\mu_i(t), \forall i$ tends to a finite constant value as $t \rightarrow \infty$.

Now we turn to prove that $\mathbf{u} \rightarrow \mathbf{0}_{np}$. Due to the difficulty arising from the term $\omega_i(t)$, and the second order dynamics, the proof is more complex than existing proofs for showing convergence to the consensus objective. Consider firstly \mathbf{e} and \mathbf{K} . By recalling the definitions of \mathbf{e}_i and the trigger function f_i , we observe that $\|\mathbf{e}\|^2 \leq \beta \|\mathbf{v}\|^2 + \bar{\omega}(t), \forall t$. We concluded above that $\lim_{t \rightarrow \infty} \|\mathbf{v}\|, \bar{\omega}(t) = 0$ which implies that $\lim_{t \rightarrow \infty} \mathbf{e} = \mathbf{0}_{np}$. Recalling the definition of \mathbf{K} above (13), and the fact that $\mu_i, \forall i$ tends to a constant value as $t \rightarrow \infty$, we conclude that $\lim_{t \rightarrow \infty} \mathbf{K} = \bar{\mathbf{K}}$ where $\bar{\mathbf{K}}$ is some finite constant matrix. Rewrite the second equation of (13) as

$$\dot{\mathbf{v}} = \mathbf{f}(t) + \mathbf{r}(t) \quad (17)$$

where $\mathbf{f}(t) = -\mathbf{M}(\mathbf{q})^{-1}(\mathbf{L}_{22} \otimes \mathbf{I}_p)\mathbf{u}$ and $\mathbf{r}(t) = -\mathbf{M}(\mathbf{q})^{-1}[\mathbf{C}(\mathbf{q}, \mathbf{v})\mathbf{v} + \mathbf{K}\mathbf{v} + \mathbf{e}]$ are both vector functions. Since $\lim_{t \rightarrow \infty} \mathbf{v}, \mathbf{e} = \mathbf{0}_{np}$, $\bar{\mathbf{K}}$ is finite, and \mathbf{M}, \mathbf{C} are bounded according to Properties P2 and P3, it is obvious that $\lim_{t \rightarrow \infty} \mathbf{r}(t) = \mathbf{0}_{np}$. Then by integrating both sides of (17) from t to $t + \Delta$, where Δ is a finite positive constant and $t \geq 0$, we obtain

$$\mathbf{v}(t + \Delta) - \mathbf{v}(t) = \int_t^{t+\Delta} \mathbf{f}(s)ds + \int_t^{t+\Delta} \mathbf{r}(s)ds \quad (18)$$

This implies that there holds

$$\left\| \int_t^{t+\Delta} \mathbf{f}(s)ds \right\| \leq \|\mathbf{v}(t + \Delta) - \mathbf{v}(t)\| + \left\| \int_t^{t+\Delta} \mathbf{r}(s)ds \right\| \quad (19)$$

Consider the term $\left\| \int_t^{t+\Delta} \mathbf{f}(s)ds \right\|$. By applying **Theorem 1**, we conclude that there holds

$$\left\| \int_t^{t+\Delta} \mathbf{f}(s)ds \right\| \leq \Delta \|\mathbf{f}(t + \theta(t))\|$$

where $\theta(t) \in (0, \Delta)$. Subtracting $\Delta \|\mathbf{f}(t)\|$ from the both sides of the above inequality yields

$$\left\| \int_t^{t+\Delta} \mathbf{f}(s)ds \right\| - \Delta \|\mathbf{f}(t)\| \leq \Delta (\|\mathbf{f}(t + \theta(t))\| - \|\mathbf{f}(t)\|)$$

Considering the above right hand side, we observe that $\Delta (\|\mathbf{f}(t + \theta(t))\| - \|\mathbf{f}(t)\|) \leq \Delta \|\mathbf{f}(t + \theta(t)) - \mathbf{f}(t)\| = \Delta \left\| \int_t^{t+\theta(t)} \dot{\mathbf{f}}(s)ds \right\|$, which implies that

$$\left\| \int_t^{t+\Delta} \mathbf{f}(s)ds \right\| - \Delta \|\mathbf{f}(t)\| \leq \Delta \left\| \int_t^{t+\theta(t)} \dot{\mathbf{f}}(s)ds \right\| \quad (20)$$

Note that $d(\mathbf{M}^{-1})/dt = -\mathbf{M}^{-1}\dot{\mathbf{M}}\mathbf{M}^{-1}$ because $d(\mathbf{M}^{-1}\mathbf{M})/dt = \mathbf{M}^{-1}\dot{\mathbf{M}} + (d(\mathbf{M}^{-1})/dt)\mathbf{M} = \mathbf{0}$. From Properties P3 and P4, we observe that $\lim_{t \rightarrow \infty} \|\dot{\mathbf{M}}\| \leq 2k_C \|\mathbf{v}\| = 0$. Observe that

$$\dot{\mathbf{f}} = - \left(\frac{d(\mathbf{M}(\mathbf{q})^{-1})}{dt} (\mathbf{L}_{22} \otimes \mathbf{I}_p)\mathbf{v} + \mathbf{M}(\mathbf{q})^{-1}(\mathbf{L}_{22} \otimes \mathbf{I}_p)\dot{\mathbf{v}} \right)$$

We proved below (16) that \mathbf{u} is bounded and $\lim_{t \rightarrow \infty} \mathbf{v} = \mathbf{0}_{np}$. Recall also that $\|\mathbf{M}(\mathbf{q})^{-1}\|$ is bounded according to Property P2. It follows that $\lim_{t \rightarrow \infty} \|\dot{\mathbf{f}}\| = 0$ which implies that $\left\| \int_t^{t+\theta(t)} \dot{\mathbf{f}}(s)ds \right\| = 0$ since $\theta(t) \in (0, \Delta)$. The inequality (20) then implies that $\lim_{t \rightarrow \infty} \left\| \int_t^{t+\Delta} \mathbf{f}(s)ds \right\| = \Delta \|\mathbf{f}(t)\|$. By substituting this into the left hand side of (19), we obtain

$$\Delta \|\mathbf{f}(t)\| \leq \|\mathbf{v}(t + \Delta) - \mathbf{v}(t)\| + \left\| \int_t^{t+\Delta} \mathbf{r}(s)ds \right\| \quad (21)$$

as $t \rightarrow \infty$. Immediately above (18), we showed that $\lim_{t \rightarrow \infty} \mathbf{r} = \mathbf{0}_{np}$. In addition, $\lim_{t \rightarrow \infty} \mathbf{v} = \mathbf{0}_{np}$ and Δ is a positive constant. We conclude that $\lim_{t \rightarrow \infty} \|\mathbf{v}(t + \Delta) - \mathbf{v}(t)\| + \left\| \int_t^{t+\Delta} \mathbf{r}(s)ds \right\| = 0$, which according to (21) implies that $\lim_{t \rightarrow \infty} \|\mathbf{f}(t)\| = 0$. By recalling that $\mathbf{f}(t) = -\mathbf{M}(\mathbf{q})^{-1}(\mathbf{L}_{22} \otimes \mathbf{I}_p)\mathbf{u}$, we conclude $\lim_{t \rightarrow \infty} \mathbf{u} = \mathbf{0}_{np}$ since both $\mathbf{M}(\mathbf{q})^{-1}$ and \mathbf{L}_{22} are both positive definite. It is obvious that $\lim_{t \rightarrow \infty} \mathbf{u}, \mathbf{v} = \mathbf{0}_{np}$ implies the leader-follower objective is asymptotically achieved.

2) *Absence of Zeno behaviour*: According to **Definition 1**, we can prove that Zeno behaviour does not occur for $t \in [0, b]$ by showing that for all $k \geq 0$ there holds $t_{k+1}^i - t_k^i \geq \xi$ where $\xi > 0$ is a strictly positive constant.

Let ξ_i denote the lower bound of the inter-event interval $t_{k+1}^i - t_k^i$ for agent i , i.e. $t_{k+1}^i - t_k^i \geq \xi_i, \forall k : t_k^i \in [0, b]$. In this part of the proof, we show that ξ_i is strictly positive for $k < \infty$ and thus no Zeno behaviour can occur. From the definition of $\mathbf{e}_i(t)$ in (9) and the fact that $\mathbf{z}_i(t_k^i)$ is a constant, we observe that the derivative of $\|\mathbf{e}_i(t)\|$ with respect to time satisfies

$$\frac{d}{dt} \|\mathbf{e}_i(t)\| \leq \|\dot{\mathbf{z}}_i(t)\| \quad (22)$$

where $\dot{\mathbf{z}}_i(t) = \sum_{j=0}^n a_{ij}(\dot{\mathbf{q}}_i(t) - \dot{\mathbf{q}}_j(t)) + \dot{\mu}_i(t)\dot{\mathbf{q}}_i(t) + \mu_i(t)\dot{\mathbf{q}}_i(t)$, $i = 1, \dots, n$. Note that it is straightforward to conclude $\dot{\mathbf{q}}_i(t), \ddot{\mathbf{q}}_i(t), \dot{\mu}_i(t), \mu_i(t)$ are bounded according to the arguments in *Part 1*). This implies $\dot{\mathbf{z}}_i(t)$ is bounded. By letting a positive constant B_e represent the upper bound of $\|\dot{\mathbf{z}}_i(t)\|$, we obtain

$$\frac{d}{dt} \|\mathbf{e}_i(t)\| \leq B_e$$

It follows that

$$\|\mathbf{e}_i(t)\| \leq \int_{t_k^i}^t B_e dt = B_e(t - t_k^i) \quad (23)$$

for $t \in [t_k^i, t_{k+1}^i)$ and for any k . It is obvious that the next event time t_{k+1}^i is determined both by the changing rate of $\|e_i(t)\|$ and by the value of the comparison term $\beta_i \|z_i(t)\|^2 + \mu_i(t)$ at t_{k+1}^i . Moreover, t_{k+1}^i is the time that

$$\|e_i(t)\|^2 = \beta_i \|v_i(t)\|^2 + \omega_i(t), \quad t > t_k^i \quad (24)$$

holds. In Part 1) we conclude that global state variable $v(t) \rightarrow \mathbf{0}_{np}$ as $t \rightarrow \infty$ but notice that in the evolution of the system (13), the state variable $v_i(t)$ may be equal to $\mathbf{0}_p$ instantaneously ($v_i(t)$ is a component of $v(t)$) may also hold at t_{k+1}^i . However, this does not imply leader-follower consensus is reached since $\dot{v}_i(t)$ can be non-zero at t_{k+1}^i . We refer to such points as ‘‘zero-crossing points’’ for convenience. Here we provide Fig. 2 to show the trigger performance at the zero-crossing points of $v_i(t)$ when $\omega_i(t) = 0$. It is observed that dense trigger behaviour occurs whenever $v_i(t)$ crosses zero. Theoretically, it can be proved that Zeno behaviour takes place at those zero-crossing points. We refer interested readers to [32] with detail arguments of the Zeno triggering issues at zero-crossing points.

Now we return to the trigger time interval analysis. By recalling (24), we conclude that at t_{k+1}^i , the triggering of the event can only occur according to the following two cases:

- Case 1: If $\|v_i(t_{k+1}^i)\| \neq 0$, the equality $\|e_i(t_{k+1}^i)\| = \beta_i \|v_i(t_{k+1}^i)\|^2 + \omega_i(t_{k+1}^i)$ is satisfied.
- Case 2: If $\|v_i(t_{k+1}^i)\| = 0$, the equality $\|e_i(t_{k+1}^i)\| = \omega_i(t_{k+1}^i)$ is satisfied.

Compare the above two cases, and note that $\|v_i(t_{k+1}^i)\| > 0$ for any $\|v_i(t_{k+1}^i)\| \neq 0$. By recalling that $e_i(t)$ is equal to zero at t_k^i , it is straightforward to conclude that it takes longer for the quantity $\|e_i(t)\|^2$ to increase to be equal to the quantity $\beta_i \|v_i(t_{k+1}^i)\|^2 + \omega_i(t_{k+1}^i)$ (i.e. Case 1) than to increase to be equal to the quantity $\omega_i(t_{k+1}^i)$ (i.e. Case 2) and thus trigger an event and resetting $e_i(t)$. This implies that $\xi_{Case 2} < \xi_{Case 1}$ and proving that there exists a strictly positive $\xi_{Case 2}$ allows us to draw the conclusion that no Zeno behaviour occurs. According to (23), we have

$$B_e \xi_{Case 2} \geq \omega_i(t) = \exp(-\kappa_i(t_k^i + \xi_{Case 2}))$$

This implies that the inter-event time $\xi_{Case 2}$ is lower bounded by the solution of the following equation

$$B_e \xi_{Case 2} = \exp(-\kappa_i(t_k^i + \xi_{Case 2})) \quad (25)$$

The solution is time-dependent and strictly positive for any finite time since B_e is strictly positive and upper bounded. Zeno behaviour is thus excluded for all agents. \square

Remark 3. The reader will have noticed the complexity and length of argument required to go from concluding $\lim_{t \rightarrow \infty} v = \mathbf{0}_{np}$ below (16), to concluding $\lim_{t \rightarrow \infty} u = \mathbf{0}_{np}$ below (21). The key reason is the combination of second-order dynamics and the non-autonomous nature of the networked system (13) resulting from the offset term $\omega_i(t)$ in the trigger function (10). The authors in [22] use a similar trigger function with the same offset term, and claim that $\lim_{t \rightarrow \infty} v = \mathbf{0}_{np}$ implies that $\lim_{t \rightarrow \infty} \dot{v} = \mathbf{0}_{np}$. This is not correct since the system is non-autonomous. The paper [33] uses a trigger function without the offset term, and thus they

are able to avoid the non-autonomous issue. However, the lack of the offset term can yield Zeno behaviour, something which was not recorded by [33]. We explore the use of the offset term for avoiding Zeno behaviour in the next section.

Remark 4. Unfortunately, we cannot find a constant lower bound for the inter-event time interval. The lower bound $\xi_{Case 2}$ found by solving (25) is still time-dependent and tends to zero as $t \rightarrow \infty$. The avoidance of Zeno behaviour depends on the exponential decay offset completely and the trigger performance when $t \rightarrow \infty$ is not discussed in the theoretical analysis. However, we note that the state-dependent term in (10) provides a performance advantage when $t \rightarrow \infty$ due to its own specific effects and should not be removed. We will provide detail explanations for the advantages of our proposed trigger function (10) in the following subsection.

B. Discussions on the chosen of trigger functions

In this subsection, we provide discussions regarding the trigger performance of controller (8) under the following three trigger functions

- State-dependent trigger function (SDTF)

$$f_i = \|e_i(t)\| - \beta_i \|v_i(t)\| \quad (26)$$

- Time-dependent trigger function (TDTF)

$$f_i = \|e_i(t)\| - \kappa_i \exp(-\varepsilon_i t) \quad (27)$$

- Mixed trigger function (MTF), which is the proposed (10)

$$f_i = \|e_i(t)\|^2 - \beta_i \|v_i(t)\|^2 - \kappa_i \exp(-\varepsilon_i t) \quad (28)$$

from both the viewpoints of theoretical analysis and numerical simulations. In doing so, we highlight the advantages of our proposed trigger function (10). Note that it is hard, but not impossible, to observe the zero-crossing phenomenon for $v_i(t) \in \mathbb{R}^p, p \geq 2$ (i.e. when $v_i(t) = \mathbf{0}_p$ occurs, Zeno behaviour is observed as discussed in the proof of Theorem 3 and in [32]). This is because each entry of $v_i(t)$ must be simultaneously equal to 0. For purposes of illustration, in this subsection we therefore simulate using dynamics of a one-arm mechanic manipulator ($v_i(t) \in \mathbb{R}^1$). The dynamics are described by equation 3.5 in [3]. For all simulations presented in this subsection, we set a constant step size in MATLAB to be 0.00005 seconds (the numerical accuracy of the simulation) and the running time to be 30 seconds. In order to compare performance, we require the following two definitions

Definition 2 (Minimum Inter-Event Time for Agent i). For $j = \{SDTF, TDTF, MTF\}$, and for $i = \{1, \dots, n\}$ define the minimum inter-event time for Agent i Δ_j^i as $\Delta_j^i \triangleq \min_k t_{k+1}^i - t_k^i$.

Definition 3 (Infimum Time of Δ_j For Agent i). For $j = \{SDTF, TDTF, MTF\}$, and for $i = \{1, \dots, n\}$, define the ‘‘infimum time of Δ_j for Agent i ’’ as $t_{\Delta_j^i} \triangleq \inf_{t_k^i} t_k^i : t^{k+2} - t_{k+1}^i = t_k^{k+1} - t_k^i = \Delta_j^i, \forall k$.

In other words, for Agent i , $t_{\Delta_j^i}$ is the infimum of all event times $t_k^i, \forall i$ such that the inter-event time between consecutive

events $k + 1$ and $k + 2$ is equal to the minimum inter-event time Δ_j^i . If there are multiple consecutive events with inter-event time $\Delta_j^i > 0$ then we call this a *dense triggering of events*. Note that because $\Delta_j^i > 0$, dense triggering is not Zeno behaviour, but is nevertheless undesirable.

Due to space limitations and the similarity of the proofs, we omit the proofs of convergence of system (11) under trigger functions (26) and (27). Figures 3 and 4 illustrate the controller (8) using SDTF (26), and TDTF (27), respectively. The figures show rendezvous of the generalized coordinates, the evolutions of comparison terms ($\beta_i \|v_i(t)\|$ in SDTF and $\kappa_i \exp(-\epsilon_i t)$ in TDTF) and event times. Figure 5 shows the performance of controller (8) using MTF. We also provide three tables to compare the trigger performance when using SDTF, TDTF and MTF. Table I records the total number of events which occur when using the three different trigger functions. Table II records the minimum inter-event time, Δ_j^i . Table III records the infimum time value, $t_{\Delta_j^i}$, which was defined in Definition 3 above.

Note that the SDTF and TDTF are widely adopted in event-based multi-agent consensus literature. We hereby review and illustrate the advantages and disadvantages regarding the trigger performance by separately using SDTF and TDTF.

1) *SDTF*: The papers [11], [13], [21], [23], [34] used SDTF to determine the event times. The disadvantage of adopting state-dependent trigger function is that Zeno behaviour can occur when the local state-dependent term crosses zero at a finite time value as indicated in [32] (i.e. in (26), the term $v_i(t) = 0$ instantaneously, for $t < \infty$). According to the first column of Table II, the minimum inter-event time is $\Delta_{\text{SDTF}}^i = 0.00005$ seconds, for all i , which is equal to the fixed time step of the MATLAB simulations. As shown in [32], Zeno behaviour will occur at these instants. From the first column of Table III and the second sub-graph of Fig. 3, we observe that Zeno behaviour occurs at the time instants that $v_i(t)$ crosses 0, which supports the conclusion of Zeno behaviour. However, according to the arguments in [11], [32], if each agent uses SDTF, then at any time t , there exists at least one agent for which the next inter-event interval is strictly positive at any time t . In other words, for all $t \in [0, \infty)$, some agents may exhibit Zeno behaviour, *but at least one agent will be Zeno free*.

2) *TDTF*: In [12], [35], [36], by using carefully-designed TDTF (typically the decay rate of $\exp(-\epsilon_i t)$ in (27) must be upper bounded), a strictly positive and *constant lower bound* on the inter-event time interval for each agent can be obtained. However, the use of the TDTF has the following two limitations: 1) the applied system has to be exponentially stable, and 2) accurate information (agent's dynamic model and network topology) is required to design the decay rate of $\exp(-\epsilon_i t)$. We emphasise that the use of TDTF with arbitrary decay rate for $\exp(-\epsilon_i t)$ is enough to exclude Zeno behaviour (see the second part of the proof of **Theorem 3**). However, if the decay rate is not selected to be sufficiently slow, the lower bound on the inter-event time cannot be guaranteed to be constant, but instead becomes time dependent. This results in dense triggering behaviour as consensus is almost reached, i.e. multiple events occur in a very short time interval (see Fig.

4). From the second columns of Table II and Table III, it is observed that Δ_j^i occurs around 29s, for all i , which is when the system is close to consensus. Note that dense triggering as $t \rightarrow \infty$ is not Zeno behaviour (See Definition 1). However, it can be observed from Table I that unsuitably chosen trigger function will introduce a large amount of events, which is obviously undesirable.

3) *MTF*: According to Table I, it is straightforward to conclude that using a MTF shows the best trigger performance with the least number of total events. According to Table I, using MTF also shows that the minimum inter-event time, Δ_j^i is greater than the constant MATLAB step size of 0.00005 seconds, which indicates Zeno behaviour is excluded. These observations reveal that MTF is able to combine the advantages of using SDTF and TDTF separately, i.e., the exclusion of Zeno behaviour in finite time (TDTF) and guarantee that dense triggering does not occur as consensus is reached (SDTF). However, a thorough analysis to find a *constant* lower bound on Δ_j^i when using MTF remains an open challenge (we can find a time-dependent bound).

Remark 5. *The work [37], [38] also use MTF. However, the authors design the evolution speeds of the exponential functions using exact knowledge of agent dynamic models and the graph topology. The effects of adding state-dependent terms to the trigger functions were not well-addressed by the authors of [37], [38].*

IV. MODEL-INDEPENDENT CONTROLLER ON DIRECTED GRAPH

In this section, we propose and analyse a distributed event-triggered model-independent algorithm to achieve leader-follower consensus on a directed network where each fully-actuated agent has self-dynamics described by the Euler-Lagrange equation. For design of the control laws, the following assumption is required.

Assumption 2 (Limited Use of Centralised Design). *Three parameters in the algorithm in this Section must be designed to exceed several lower bounding inequalities. These inequalities require knowledge of the constants k_m, k_M, k_C defined in the properties P2 and P3. We therefore assume these constants are known to the designer.*

A. Main Result

Let the triggering time sequence of agent i be $t_0^i, t_1^i, \dots, t_k^i, \dots$ with $t_0^i := 0$. Consider a model-independent, event-triggered algorithm for the i^{th} follower agent of the form

$$\tau_i(t) = - \sum_{j \in \mathcal{N}_i} a_{ij} \left((\mathbf{q}_i(t_k^i) - \mathbf{q}_j(t_k^i)) + \mu (\dot{\mathbf{q}}_i(t_k^i) - \dot{\mathbf{q}}_j(t_k^i)) \right) \quad t \in [t_k^i, t_{k+1}^i) \quad (29)$$

where a_{ij} is the weighted (i, j) entry of the adjacency matrix \mathcal{A} associated with the weighted directed graph \mathcal{G} . The control gain scalar $\mu > 0$ is universal to all agents. To ensure the control objective is achieved, μ must be designed to satisfy several inequalities, which will be detailed below. Note that if the leader is a neighbour of agent i then for $j = 0$ we have

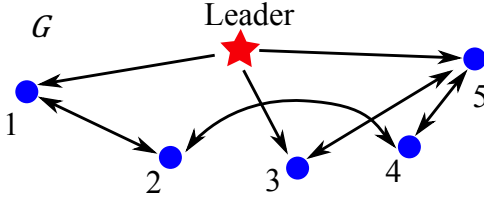


Fig. 1. Graph topology used in simulations

TABLE II
MINIMUM INTER-EVENT TIME Δ_j^i UNDER THREE TRIGGER FUNCTIONS

	State-dependent	Time-dependent	Mixed
Agent 1	0.00005	0.00005	0.0388
Agent 2	0.00005	0.00005	0.0235
Agent 3	0.00005	0.00005	0.0010
Agent 4	0.00005	0.00005	0.0037
Agent 5	0.00005	0.00005	0.0006

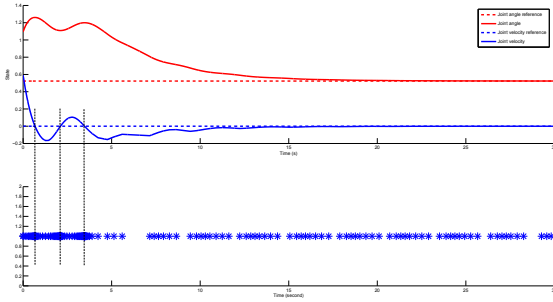


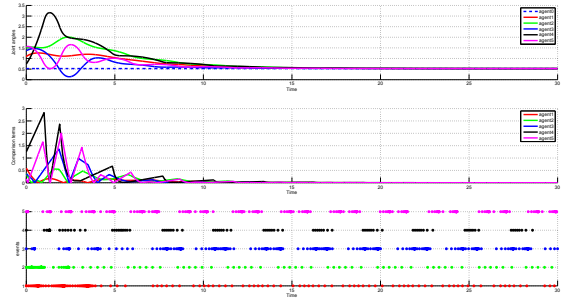
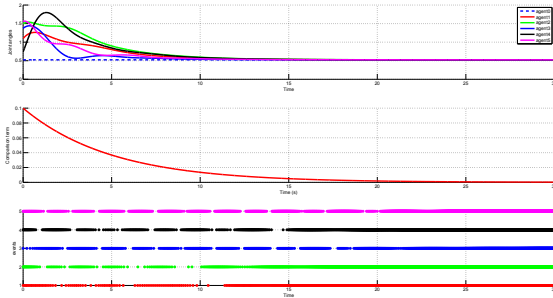
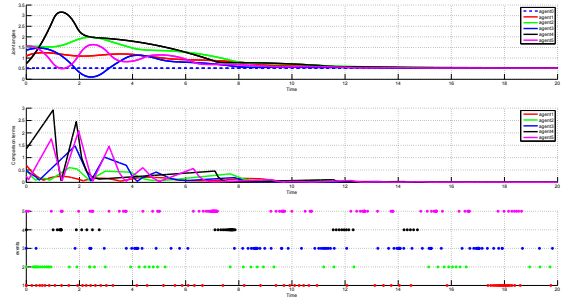
Fig. 2. Top: the evolutions of the generalized coordinate and velocity of agent 1. Bottom: the trigger event times of agent 1

TABLE I
NUMBER OF EVENTS FOR THREE DIFFERENT TRIGGER FUNCTIONS

	State-dependent	Time-dependent	Mixed
Agent 1	259	5581	74
Agent 2	184	8106	63
Agent 3	575	2251	168
Agent 4	94	7365	101
Agent 5	438	3845	200
Total	1550	27148	606

TABLE III
THE INFIMUM TIME OF $\Delta_j, t_{\Delta_j^i}$ AS DEFINED IN DEFINITION 3

	State-dependent	Time-dependent	Mixed
Agent 1	0.6736	29.8177	18.0246
Agent 2	0.3042	29.6469	2.3991
Agent 3	0.4722	29.8398	14.0583
Agent 4	1.3219	29.6458	1.3182
Agent 5	0.0798	29.9830	15.435

Fig. 3. Performance of controller (8) using SDTF (26). We set $\beta_i = 2.4$. From top to bottom: 1) the rendezvous of the generalized coordinates; 2) the evolution of $\beta_i \|v_i(t)\|$; 3) event times for each agent.Fig. 4. Performance of controller (8) using TDTF (27). We set $\kappa_i \exp(-\varepsilon_i t) = 0.1 \exp(-0.2t)$. From top to bottom: 1) the rendezvous of the generalized coordinates; 2) the evolution of $\kappa_i \exp(-\varepsilon_i t)$; 3) event times for each agent.Fig. 5. Performance of controller (8) with MTF (28). We set $\beta_i = 2.4$ and $\kappa_i \exp(-\varepsilon_i t) = 0.1 \exp(-0.2t)$. From top to bottom: 1) the rendezvous of the generalized coordinates; 2) the evolution of $\beta_i \|v_i(t)\| + \kappa_i \exp(-\varepsilon_i t)$; 3) event times for each agent.

$\mu(\dot{q}_i(t_k^i) - \dot{q}_0(t_k^i)) = \mu(\dot{q}_i(t_k^i))$, which is simply a damping term.

Define a new variable

$$z_i(t) = \sum_{j \in \mathcal{N}_i} a_{ij} \left((q_i(t) - q_j(t)) + \mu(\dot{q}_i(t) - \dot{q}_j(t)) \right)$$

We define a state mismatch for agent i between consecutive event times t_k^i and t_{k+1}^i as follows:

$$e_i(t) = z_i(t_k^i) - z_i(t) \quad (30)$$

event times t_k^i and t_{k+1}^i as follows:

for $t \in [t_k^i, t_{k+1}^i)$.

The trigger function is proposed as follows:

$$f_i(e_i(t)) = \|e_i(t)\|^2 - \mu^{-2}\beta_1^2 \left\| \sum_{j \in \mathcal{N}_i} a_{ij}(\mathbf{q}_i(t) - \mathbf{q}_j(t)) \right\|^2 - \beta_2^2 \left\| \sum_{j \in \mathcal{N}_i} a_{ij}(\mathbf{v}_i(t) - \mathbf{v}_j(t)) \right\|^2 - \omega_i(t) \quad (31)$$

where $\omega_i(t) = a_i \exp(-\kappa_i t)$ where $a_i, \kappa_i > 0$. The parameters β_1 and β_2 are to be determined in the sequel. The k^{th} event for agent i is triggered as soon as the trigger condition $f_i(e_i(t)) = 0$ is fulfilled at $t = t_k^i$. For $t \in [t_k^i, t_{k+1}^i)$, the control input is $\tau_i(t) = \tau_i(t_k^i)$; the control input is updated when the next event is triggered. Furthermore, every time an event is triggered, and in accordance with their definitions, the measurement error $e_i(t)$ is reset to be equal to zero and thus the trigger function assumes a negative value. One can immediately observe that for all t

$$\|e_i(t)\|^2 \leq \mu^{-2}\beta_1^2 \left\| \sum_{j \in \mathcal{N}_i} a_{ij}(\mathbf{q}_i(t) - \mathbf{q}_j(t)) \right\|^2 + \beta_2^2 \left\| \sum_{j \in \mathcal{N}_i} a_{ij}(\mathbf{v}_i(t) - \mathbf{v}_j(t)) \right\|^2 + \omega_i(t)$$

and note that $\sum_{j \in \mathcal{N}_i} a_{ij}(\mathbf{q}_i(t) - \mathbf{q}_j(t)) = \sum_{j \in \mathcal{N}_i} a_{ij}[(\mathbf{q}_i(t) - \mathbf{q}_0) - (\mathbf{q}_j(t) - \mathbf{q}_0)] = \mathbf{l}_i^\top \mathbf{u}$ where \mathbf{l}_i^\top is the i^{th} row of \mathcal{L}_{22} . Likewise, $\sum_{j \in \mathcal{N}_i} a_{ij}(\mathbf{v}_i(t) - \mathbf{v}_j(t)) = \mathbf{l}_i^\top \mathbf{v}$. The stacked column vector $\mathbf{e} = [\mathbf{e}_1^\top, \dots, \mathbf{e}_n^\top]^\top$ then has the following property

$$\begin{aligned} \|\mathbf{e}\|^2 &= \sum_{i=1}^n \|e_i(t)\|^2 \\ &\leq \sum_{i=1}^n \left(\mu^{-2}\beta_1^2 \|\mathbf{l}_i^\top \mathbf{u}\|^2 + \beta_2^2 \|\mathbf{l}_i^\top \mathbf{v}\|^2 + \omega_i(t) \right) \end{aligned} \quad (32)$$

It is straightforward to verify that $\sum_{i=1}^n \|\mathbf{l}_i^\top \mathbf{u}\|^2 = \|\mathcal{L}_{22} \mathbf{u}\|^2$, and $\sum_{i=1}^n \|\mathbf{l}_i^\top \mathbf{v}\|^2 = \|\mathcal{L}_{22} \mathbf{v}\|^2$. It then follows that

$$\|\mathbf{e}\|^2 \leq \mu^{-2}\beta_1^2 \|\mathcal{L}_{22} \mathbf{u}\|^2 + \beta_2^2 \|\mathcal{L}_{22} \mathbf{v}\|^2 + \bar{\omega}(t)^2 \quad (33)$$

$$\|\mathbf{e}\| \leq \mu^{-1}\beta_1 \|\mathcal{L}_{22}\| \|\mathbf{u}\| + \beta_2 \|\mathcal{L}_{22}\| \|\mathbf{v}\| + \bar{\omega}(t) \quad (34)$$

where $\bar{\omega}(t) = (\sum_{i=1}^n \omega_i(t))^{\frac{1}{2}}$

It is obvious that

$$\boldsymbol{\tau}_i(t) = \mathbf{z}_i(t) + \mathbf{e}_i(t)$$

Applying control law (29) to each agent we can express the networked system using the new variables \mathbf{u}, \mathbf{v} as below

$$\mathbf{M}(\mathbf{q})\dot{\mathbf{v}} + \mathbf{C}(\mathbf{q}, \mathbf{v})\mathbf{v} + (\mathcal{L}_{22} \otimes \mathbf{I}_p)(\mathbf{u} + \mu\mathbf{v}) + \mathbf{e} = \mathbf{0} \quad (35)$$

and expressed as the non-autonomous system

$$\begin{aligned} \dot{\mathbf{u}} &= \mathbf{v} \\ \dot{\mathbf{v}} &= -\mathbf{M}(\mathbf{q})^{-1} [\mathbf{C}(\mathbf{q}, \mathbf{v})\mathbf{v} + (\mathcal{L}_{22} \otimes \mathbf{I}_p)(\mathbf{u} + \mu\mathbf{v}) + \mathbf{e}] \end{aligned} \quad (36)$$

By using arguments like those of usual Lyapunov theory, we will be able to prove the stability of (36). Before we present the main theorem of this section, we state a mild assumption used *only in this Section*.

Assumption 3. *All possible initial conditions lie in some fixed but arbitrarily large set, which is known a priori. In particular,*

$\|\mathbf{u}_i(0)\| \leq k_a/\sqrt{n}$ and $\|\mathbf{v}_i(0)\|_2 \leq k_b/\sqrt{n}$, where k_a, k_b are known a priori.

This assumption is entirely reasonable; many Euler-Lagrange systems will have an expected operating range for \mathbf{q} and $\dot{\mathbf{q}}$.

Theorem 4. *Suppose that each follower agent with dynamics (6), under Assumption 1, employs the controller (29) with trigger function (31). Suppose further that the directed graph \mathcal{G} contains a directed spanning tree, with the leader agent 0 as the root node (and thus with no incoming edges). Then there exists a sufficiently large μ , and sufficiently small β_1, β_2 which ensures that the leader-follower consensus objective is achieved semi-globally exponentially fast.*

Proof. The proof of this theorem is lengthy and complex due to the combination of the highly nonlinear Euler-Lagrange dynamics, the directed graph, and the event-based controller. To ensure the presentation of results is not disrupted, we move the proof to Appendix B. \square

V. ADAPTIVE, MODEL-DEPENDENT CONTROLLER ON DIRECTED NETWORK

In this section, we propose an adaptive, distributed event-triggered controller to achieve leader-follower consensus for a directed network of Euler-Lagrange agents. This allows for uncertain parameters in each agent, e.g. the mass of a robotic manipulator arm, and includes the gravitational forces.

A. Main Result

Before we present the main results, we introduce variables which allow us to rewrite the multi-agent system in a way which facilitates stability analysis. A lemma on stability is also provided. To begin, we introduce the following auxiliary variables \mathbf{q}_{ri} and \mathbf{s}_i , which appeared in [7], [39] studying leader-follower problems in directed Euler-Lagrange networks. Define

$$\dot{\mathbf{q}}_{ri}(t) = -\alpha \sum_{j=0}^n a_{ij}(\mathbf{q}_i(t) - \mathbf{q}_j(t)), \quad (37)$$

$$\begin{aligned} \mathbf{s}_i(t) &= \dot{\mathbf{q}}_i(t) - \dot{\mathbf{q}}_{ri}(t) = \dot{\mathbf{q}}_i(t) + \alpha \sum_{j=0}^n a_{ij}(\mathbf{q}_i(t) - \mathbf{q}_j(t)), \\ & \quad i = 1, \dots, n \end{aligned} \quad (38)$$

where α is a positive constant, a_{ij} is the weighted (i, j) entry of the adjacency matrix \mathbf{A} associated with the directed graph \mathcal{G} that characterises the sensing flows among the n followers. According to **Lemma 5**, one can then verify that the compact form of (38) can be written as:

$$\dot{\mathbf{q}}(t) = -\alpha(\mathcal{L}_{22} \otimes \mathbf{I}_p)(\mathbf{q}(t) - \mathbf{1}_n \otimes \mathbf{q}_0) + \mathbf{s}(t) \quad (39)$$

The following lemma will later be used for stability analysis of the networked system.

Lemma 6. *(From [39]) Suppose that, for the system (39), the graph \mathcal{G} contains a directed spanning tree with the leader as the root vertex. Then system (39) is input-to-state stable with*

respect to input $s(t)$. If $s(t) \rightarrow \mathbf{0}_p$ as $t \rightarrow \infty$, then $\dot{q}_i(t) \rightarrow \mathbf{0}_p$ and $q_i(t) \rightarrow q_0$ as $t \rightarrow \infty$.

Note that the proof of the above lemma is part of the proof of **Corollary 3.7** in [39].

From P(6) and the definition of \dot{q}_{ri} , we obtain

$$M_i(q_i)\ddot{q}_{ri} + C_i(q_i, \dot{q}_i)\dot{q}_{ri} + g_i(q_i) = Y_i(q_i, \dot{q}_i, \ddot{q}_{ri}, \dot{q}_{ri})\Theta_i, \quad i = 1, \dots, n \quad (40)$$

Note that Θ_i is an unknown but constant vector for agent i . Let $\hat{\Theta}_i(t)$ be the estimate of Θ_i at time t . We update $\hat{\Theta}_i(t)$ by the following adaptation law:

$$\dot{\hat{\Theta}}_i(t) = -\Lambda_i Y_i^\top(t) s_i(t), \quad i = 1, \dots, n \quad (41)$$

where Λ_i is a symmetric positive-definite matrix.

The control algorithm is now proposed. Let the triggering time sequence of agent i be $t_0^i, t_1^i, \dots, t_k^i, \dots$ with $t_0^i := 0$. The event-triggered controller for follower agent i is designed as:

$$\tau_i(t) = -K_i s_i(t_k^i) + Y_i(t_k^i) \hat{\Theta}_i(t_k^i), \quad i = 1, \dots, n, \quad t \in [t_k^i, t_{k+1}^i) \quad (42)$$

where $K_i > 0$ is a symmetric positive definite matrix. It is observed that the control torque remains constant in the time interval $[t_k^i, t_{k+1}^i)$, i.e. $\tau_i(t)$ is a piecewise-constant function in time. From the definitions of q_{ri} and s_i , calculations show that the system in (5) can be written as

$$M_i(q_i)\dot{s}_i(t) + C_i(q_i, \dot{q}_i)s_i(t) = -K_i s_i(t_k^i) + Y_i(t_k^i) \hat{\Theta}_i(t_k^i) - Y_i(t) \Theta_i \quad (44)$$

Before the trigger function is presented, we define two types of measurement errors:

$$\begin{aligned} e_i(t) &= s_i(t_k^i) - s_i(t); \\ \varepsilon_i(t) &= Y_i(t_k^i) \hat{\Theta}_i(t_k^i) - Y_i(t) \hat{\Theta}_i(t); \end{aligned} \quad (45)$$

The trigger function is proposed as follows:

$$\begin{aligned} f_i(\varepsilon_i(t), e_i(t), \mu_i(t)) &= \|\varepsilon_i(t)\| + \lambda_{\max}(K_i) \|e_i(t)\| \\ &\quad - \frac{\gamma_i}{2} \lambda_{\min}(K_i) \|s_i(t)\| - \omega_i(t) \end{aligned} \quad (46)$$

where $0 < \gamma_i < 1$, $\omega_i(t) = \sigma_i \sqrt{\lambda_{\min}(K_i)} \exp(-\kappa_i t)$ with $\sigma_i, \kappa_i > 0$. The k^{th} event for agent i is triggered as soon as the trigger condition $f_i(\varepsilon_i(t), e_i(t)) = 0$ is fulfilled at $t = t_k^i$. For $t \in [t_k^i, t_{k+1}^i)$, the control input is $\tau_i(t) = \tau_i(t_k^i)$; the control input is updated when the next event is triggered. Furthermore, every time an event is triggered, and in accordance with their definitions, the measurement errors $\varepsilon_i(t)$ and $e_i(t)$ are reset to be equal to zero. Thus $f_i(\varepsilon_i(t), e_i(t), \omega_i(t)) \leq 0$ for all $t \geq 0$.

We now present our main result.

Theorem 5. Consider the multi-agent system (5) with control law (43). If \mathcal{G} contains a directed spanning tree with the leader as the root vertex (and thus with no incoming edges), then leader-follower consensus ($\|q_i - q_0\| \rightarrow 0$ and $\|\dot{q}_i\| \rightarrow 0$, $i = 1, \dots, n$) is globally asymptotically achieved as $t \rightarrow \infty$ and no agent will exhibit Zeno behaviour.

Proof. In this part, we focus on the stability analysis of the system (44). The proof on the exclusion of Zeno behaviour is omitted since the idea is the same with that in Part 2) of the proof of **Theorem 3**. Notice that (44) is non-autonomous in the sense that it is not self-contained (M_i, C_i depend on q_i and \dot{q}_i , respectively). However, study of a Lyapunov-like function shows leader-follower consensus is achieved.

We make use of abuse of notation by omitting the argument of time t for time-dependent functions when appropriate, e.g. q_i denotes $q_i(t)$.

Consider the following Lyapunov-like function

$$V = \frac{1}{2} \sum_{i=1}^N s_i^\top M_i(q_i) s_i + \frac{1}{2} \sum_{i=1}^N \tilde{\Theta}_i^\top \Lambda_i^{-1} \tilde{\Theta}_i \quad (47)$$

where

$$\tilde{\Theta}_i = \Theta_i - \hat{\Theta}_i \quad (48)$$

The derivative of V along the solution of (44) is

$$\begin{aligned} \dot{V} &= \frac{1}{2} \sum_{i=1}^N s_i^\top \dot{M}_i(q_i) s_i + \sum_{i=1}^N s_i^\top M_i(q_i) \dot{s}_i + \sum_{i=1}^N \tilde{\Theta}_i^\top \Lambda_i^{-1} \dot{\tilde{\Theta}}_i \\ &= \sum_{i=1}^N s_i^\top \left(\frac{1}{2} \dot{M}_i(q_i) - C_i(q_i, \dot{q}_i) \right) s_i - \sum_{i=1}^N s_i^\top K_i s_i(t_k^i) \\ &\quad + \sum_{i=1}^N s_i^\top Y_i(t_k^i) \hat{\Theta}_i(t_k^i) - \sum_{i=1}^N s_i^\top Y_i \Theta_i + \sum_{i=1}^N \tilde{\Theta}_i^\top Y_i^\top s_i \end{aligned}$$

From P(4) we have $\frac{1}{2} \dot{M}_i(q_i) - C_i(q_i)$ is skew-symmetric and with $\Theta_i = \tilde{\Theta}_i + \hat{\Theta}_i$, we obtain

$$\begin{aligned} \dot{V} &= - \sum_{i=1}^N s_i^\top K_i s_i(t_k^i) + \sum_{i=1}^N s_i^\top Y_i(t_k^i) \hat{\Theta}_i(t_k^i) \\ &\quad - \sum_{i=1}^N s_i^\top Y_i (\tilde{\Theta}_i + \hat{\Theta}_i) + \sum_{i=1}^N \tilde{\Theta}_i^\top Y_i^\top s_i \end{aligned}$$

By recalling the definition of e_i and ε_i in (45), we have

$$\dot{V} = - \sum_{i=1}^N s_i^\top K_i s_i - \sum_{i=1}^N s_i^\top K_i e_i + \sum_{i=1}^N s_i^\top \varepsilon_i$$

Since K_i is a symmetric positive definite matrix, the upper bound of \dot{V} is expressed as

$$\begin{aligned} \dot{V} &\leq - \sum_{i=1}^N \lambda_{\min}(K_i) \|s_i\|^2 + \sum_{i=1}^N \lambda_{\max}(K_i) \|s_i\| \|e_i\| \\ &\quad + \sum_{i=1}^N \|s_i\| \|\varepsilon_i\| \end{aligned}$$

Note that the trigger condition $f_i(\varepsilon_i(t), e_i(t), \omega_i(t)) = 0$ guarantees that $\|\varepsilon_i\| + \lambda_{\max}(K_i) \|e_i\| \leq \frac{\gamma_i}{2} \lambda_{\min}(K_i) \|s_i\| + \omega_i(t)$

holds throughout the evolution of system (44). By further introducing the definition of $\omega_i(t)$ in (46), we obtain

$$\begin{aligned} \dot{V} \leq & -\sum_{i=1}^N \lambda_{\min}(\mathbf{K}_i) \|\mathbf{s}_i\|^2 + \sum_{i=1}^N \frac{\gamma_i}{2} \lambda_{\min}(\mathbf{K}_i) \|\mathbf{s}_i\|^2 \\ & + \sum_{i=1}^N \sqrt{\lambda_{\min}(\mathbf{K}_i)} \|\mathbf{s}_i\| \sigma_i \exp(-\kappa_i t) \end{aligned}$$

Because there holds $|xy| \leq \frac{\gamma_i}{2} x^2 + \frac{1}{2\gamma_i} y^2, \forall x, y \in \mathbb{R}$, for $0 < \gamma_i < 1$, analysis of the right hand side of the above inequality implies that \dot{V} can be further upper bounded as

$$\dot{V} \leq \sum_{i=1}^N (\gamma_i - 1) \lambda_{\min}(\mathbf{K}_i) \|\mathbf{s}_i\|^2 + \sum_{i=1}^N \frac{\sigma_i^2}{2\gamma_i} \exp(-2\kappa_i t) \quad (49)$$

Integrating both sides of (49) for any $t > 0$ yields:

$$\begin{aligned} V + \sum_{i=1}^N (1 - \gamma_i) \lambda_{\min}(\mathbf{K}_i) \int_0^t \|\mathbf{s}_i(\tau)\|^2 d\tau \\ \leq V(0) + \sum_{i=1}^N \frac{\sigma_i^2}{4\gamma_i \kappa_i} \end{aligned} \quad (50)$$

which implies that V is bounded. Since V is bounded, according to (47), both s_i and $\tilde{\Theta}_i(t)$, for all $i \in \{1, \dots, n\}$, are bounded. Now we return to (40) and obtain that

$$\|\mathbf{Y}_i \Theta_i\| \leq \|\mathbf{M}_i\| \|\ddot{\mathbf{q}}_{ri}\| + \|\mathbf{C}_i\| \|\dot{\mathbf{q}}_{ri}\| + \|\mathbf{g}_i\|$$

By recalling that the linear system (39) is input-to-state stable and the fact that s is bounded, we conclude that \mathbf{q}_i and $\dot{\mathbf{q}}_i$ are both bounded. Because \mathbf{q}_i and $\dot{\mathbf{q}}_i$ are bounded then, from their definitions, so are $\dot{\mathbf{q}}_{ri}$ and $\ddot{\mathbf{q}}_{ri}$. Then from P(2), P(3) and P(5), the assumed properties of Euler-Lagrange equations, we have that $\|\mathbf{Y}_i\|$ is upper bounded by a positive value. From the above conclusions, it is straightforward to see that the right hand side of (44), \mathbf{M}_i , \mathbf{C}_i and \mathbf{s}_i are all bounded. We thus obtain that $\dot{\mathbf{s}}_i$ is bounded. From this, it is obvious that $\mathbf{s}_i, \dot{\mathbf{s}}_i \in L_\infty$. Turning to (50), it follows that

$$\sum_{i=1}^N (1 - \gamma_i) \lambda_{\min}(\mathbf{K}_i) \int_0^t \|\mathbf{s}_i(\tau)\|^2 d\tau \leq V(0) + \sum_{i=1}^N \frac{\sigma_i^2}{4\gamma_i \kappa_i} \quad (51)$$

which indicates that $\int_0^t \|\mathbf{s}_i(\tau)\|^2 d\tau$ is bounded and thus $s_i \in \mathcal{L}_2$. By applying **Lemma 1**, we have that $s_i \rightarrow \mathbf{0}_p$ as $t \rightarrow \infty$. Then by applying **Lemma 6**, we conclude that $\mathbf{q}_i - \mathbf{q}_0 \rightarrow \mathbf{0}_p$ and $\dot{\mathbf{q}}_i \rightarrow \mathbf{0}_p$ as $t \rightarrow \infty$. The leader-follower objective is globally asymptotically achieved. \square

VI. SIMULATIONS

In this subsection, we will provide three simulations to respectively demonstrate the performance of the three proposed controllers in this paper for application to industrial manipulators (See Fig. 6). Although the effectiveness of controller (8) is verified in subsection III-B, the applied system is simple

TABLE IV
AGENTS' INITIAL STATES USED IN SIMULATIONS

	$q_i^{(1)}(0)$	$q_i^{(1)}(0)$	$\dot{q}_i^{(1)}(0)$	$\dot{q}_i^{(1)}(0)$
Agent 0	$\pi/6$	$\pi/3$	0.0	0.0
Agent 1	$\pi/5$	$\pi/6$	0.8	0.2
Agent 2	$\pi/6$	$\pi/4$	-0.2	0.3
Agent 3	$\pi/9$	$\pi/6$	0.6	-0.4
Agent 4	$\pi/8$	$\pi/4$	0.5	0.1
Agent 5	$\pi/9$	$\pi/6$	0.1	0.0

one-arm manipulators. In this subsection we assume that all two-link manipulators share the same dynamic models and parameters. The Euler-Lagrange equations for the i^{th} two-link manipulator is:

$$\begin{bmatrix} M_i^{11} & M_i^{12} \\ M_i^{21} & M_i^{22} \end{bmatrix} \begin{bmatrix} \ddot{q}_i^{(1)} \\ \ddot{q}_i^{(2)} \end{bmatrix} + \begin{bmatrix} C_i^{11} & C_i^{12} \\ C_i^{21} & C_i^{22} \end{bmatrix} \begin{bmatrix} \dot{q}_i^{(1)} \\ \dot{q}_i^{(2)} \end{bmatrix} + \begin{bmatrix} g_i^{(1)} \\ g_i^{(2)} \end{bmatrix} = \begin{bmatrix} \tau_i^{(1)} \\ \tau_i^{(2)} \end{bmatrix}$$

The elements in M_i , C_i matrices and g_i vector are given below:

$$\begin{aligned} M_i^{11} &= (m_1 + m_2)d_1^2 + m_2d_2^2 + 2m_2d_1d_2 \cos(q_i^{(2)}) \\ M_i^{12} &= M_i^{21} = m_2(d_2^2 + d_1d_2 \cos(q_i^{(2)})) \\ M_i^{22} &= m_2d_2^2 \\ C_i^{11} &= -m_2d_1d_2 \sin(q_i^{(2)})\dot{q}_i^{(2)} \\ C_i^{12} &= -m_2d_1d_2 \sin(q_i^{(2)})\dot{q}_i^{(2)} - m_2d_1d_2 \sin(q_i^{(2)})\dot{q}_i^{(1)} \\ C_i^{21} &= m_2d_1d_2 \sin(q_i^{(2)})\dot{q}_i^{(1)} \\ C_i^{22} &= 0 \\ g_i^{(1)} &= (m_1 + m_2)gd_1 \sin(q_i^{(1)}) + m_2gd_2 \sin(q_i^{(1)} + q_i^{(2)}) \\ g_i^{(2)} &= m_2gd_2 \sin(q_i^{(1)} + q_i^{(2)}) \end{aligned}$$

where g is the acceleration due to gravity, d_1 and d_2 are lengths of the 1st and 2nd links of the manipulator, respectively; m_1 and m_2 are mass of the 1st and 2nd of the manipulator. The physical parameters of each manipulator are selected as $g = 9.8 \text{ m/s}^2$, $d_1 = 1.5 \text{ m}$, $d_2 = 1 \text{ m}$, $m_1 = 1 \text{ kg}$, $m_2 = 2 \text{ kg}$. The initial states of each manipulator are shown in Table I. Note that in simulations 1 and 2, we assume that $g_i^{(1)}, g_i^{(2)} = 0$.

Simulation 1. This simulation will demonstrate the performance of controller (8) under trigger condition (10). The sensing graph \mathcal{G} associated with the five follower manipulators and the leader manipulator has the following weighted Laplacian

$$\mathcal{L} = \begin{bmatrix} 0 & 0 & 0 & 0 & 0 & 0 \\ -1 & 3.9 & -1.55 & 0 & -1.35 & 0 \\ -1 & -1.55 & 6.4 & -2.1 & -1.75 & 0 \\ 0 & 0 & -2.1 & 7.35 & -2.35 & -2.9 \\ 0 & -1.35 & -1.75 & -2.35 & 6.7 & -1.25 \\ 0 & 0 & 0 & -2.9 & -1.25 & 4.15 \end{bmatrix}$$

The initial value of the variable-gain scalar $\mu_i(t)$ is chosen as $\mu_i(0) = 0$. The exponential function used in trigger function (10) is selected as $\omega_i(t) = 1.8 * \exp(-0.2 * t)$. The performance of the controller is demonstrated in Fig. 7.

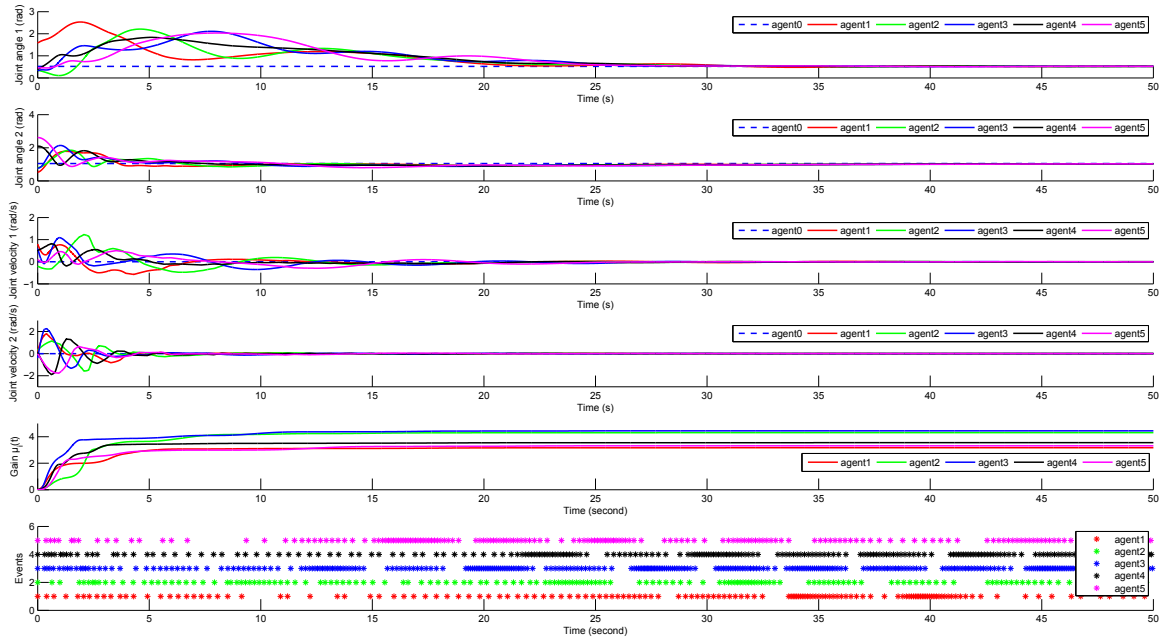


Fig. 7. Simulation results for controller (8) under trigger function (10). From top to bottom: the plots the generalized coordinates; the plots of generalised velocities of all the follower manipulators; the plot of variable gain $\mu_i(t)$; the plot of trigger events

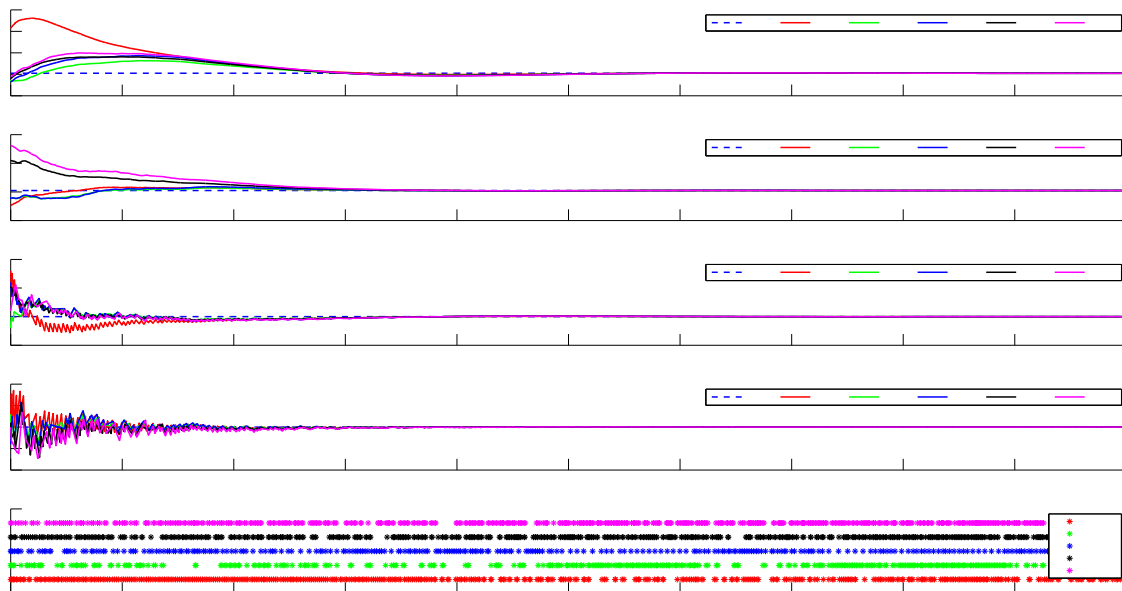


Fig. 8. Simulation results for controller (29) under trigger function (31). From top to bottom: the plots the generalized coordinates; the plots of generalised velocities of all the follower manipulators; the plot of trigger events

- [11] D. V. Dimarogonas, E. Frazzoli, and K. H. Johansson, "Distributed event-triggered control for multi-agent systems," *Automatic Control, IEEE Transactions on*, vol. 57, no. 5, pp. 1291–1297, 2012.
- [12] G. S. Seyboth, D. V. Dimarogonas, and K. H. Johansson, "Event-based

broadcasting for multi-agent average consensus," *Automatica*, vol. 49, no. 1, pp. 245–252, 2013.

- [13] Y. Fan, G. Feng, Y. Wang, and C. Song, "Distributed event-triggered control of multi-agent systems with combinational measurements," *Au-*

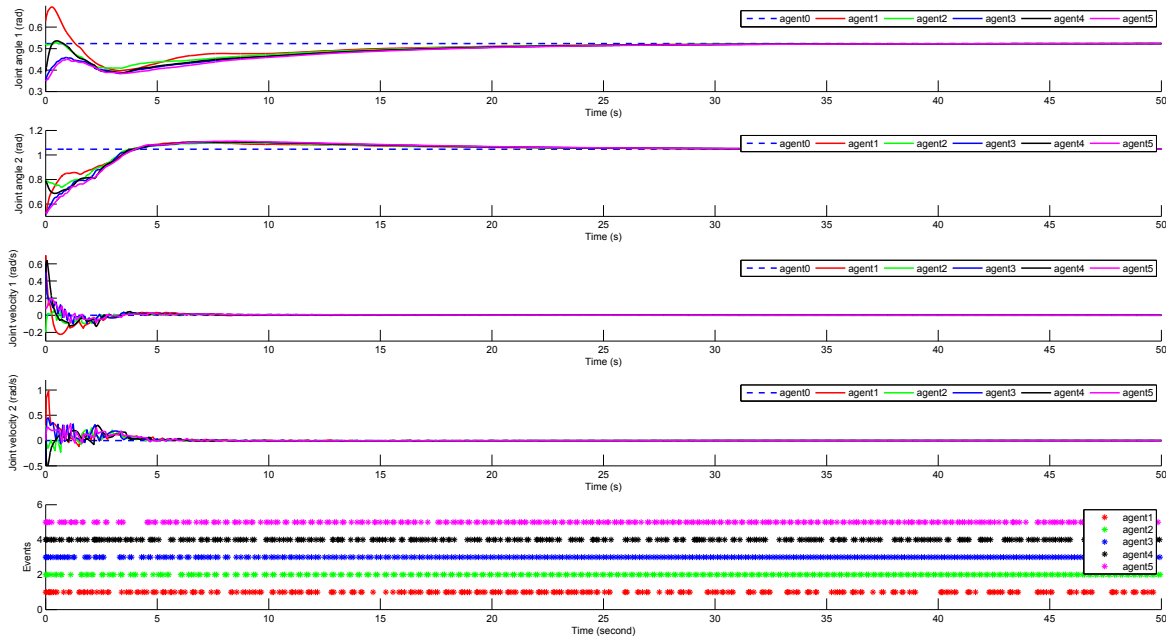


Fig. 9. Simulation results for controller (43) under trigger function (46). From top to bottom: the plots the generalized coordinates; the plots of generalised velocities of all the follower manipulators; the plot of trigger events

- tomatica*, vol. 49, no. 2, pp. 671–675, 2013.
- [14] Y. Fan, L. Liu, G. Feng, and L. Wang, “Self-triggered consensus for multi-agent systems with zero-free triggers,” *Automatic Control, IEEE Transactions on*, vol. 60, no. 10, pp. 2779 – 2784, 2015.
- [15] Q. Liu, J. Qin, and C. Yu, “Event-based multi-agent cooperative control with quantized relative state measurements,” in *Decision and Control, 2016. 55th IEEE Conference on*, pp. 2233 – 2239, IEEE, 2016.
- [16] C. Nowzari and J. Cortes, “Distributed event-triggered coordination for average consensus on weight-balanced digraphs,” *Automatica*, vol. 68, pp. 237–244, February 2016.
- [17] B. Mu, H. Li, W. Li, and Y. Shi, “Consensus for multiple euler-lagrange dynamics with arbitrary sampling periods and event-triggered strategy,” in *Intelligent Control and Automation (WCICA), 2014 11th World Congress on*, pp. 2596–2601, IEEE, 2014.
- [18] N. Huang, Z. Duan, and Y. Zhao, “Distributed consensus for multiple euler-lagrange systems: An event-triggered approach,” *Science China Technological Sciences*, vol. 59, pp. 33–44, 2016.
- [19] Z. Meng and Z. Lin, “Distributed Finite-time Cooperative Tracking of Networked Lagrange Systems via Local Interactions,” in *American Control Conference (ACC), Montréal, Canada*, pp. 4951–4956, IEEE, 2012.
- [20] J. Mei, W. Ren, and G. Ma, “Distributed Coordinated Tracking With a Dynamic Leader for Multiple Euler-Lagrange Systems,” *IEEE Transactions on Automatic Control*, vol. 56, no. 6, pp. 1415–1421, 2011.
- [21] X. Liu, C. Du, P. Lu, and D. Yang, “Decentralised consensus for multiple lagrangian systems based on event-triggered strategy,” *International Journal of Control*, vol. 89, no. 6, pp. 1111–1124, 2016.
- [22] N. Huang, Z. Duan, and Y. Zhao, “Distributed consensus for multiple Euler-Lagrange systems: An event-triggered approach,” *Science China: Technological Sciences*, vol. 59, pp. 33–44, January 2016.
- [23] E. Garcia, Y. Cao, H. Yu, P. Antsaklis, and D. Casbeer, “Decentralised event-triggered cooperative control with limited communication,” *International Journal of Control*, vol. 86, no. 9, pp. 1479–1488, 2013.
- [24] J. Mei, W. Ren, J. Chen, and B. D. Anderson, “Consensus of linear multi-agent systems with fully distributed control gains under a general directed graph,” in *IEEE 53rd Annual Conference on Decision and Control*, (Los Angeles, USA), pp. 2993–2998, IEEE, 2014.
- [25] J. Mei, W. Ren, and J. Chen, “Distributed Consensus of Second-Order Multi-Agent Systems with Heterogeneous Unknown Inertias and Control Gains Under a Directed Graph,” *IEEE Transactions on Automatic Control*, vol. 61, no. 8, pp. 2019–2034, 2016.
- [26] Z. Li and Z. Duan, *Cooperative Control of Multi-Agent Systems: A Consensus Region Approach*. CRC Press, 2014.
- [27] Q. Liu, M. Ye, J. Qin, and C. Yu, “Event-based leader-follower consensus for multiple Euler-Lagrange systems with parametric uncertainties,” in *Proceedings of IEEE 55th Annual Conference on Decision and Control (CDC), Las Vegas, USA*, pp. 2240–2246.
- [28] W. Rudin *et al.*, *Principles of mathematical analysis*, vol. 3. McGraw-Hill New York, 1964.
- [29] R. A. Horn and C. R. Johnson, *Matrix Analysis*. Cambridge University Press, New York, 2012.
- [30] P. A. Ioannou and B. Fidan, *Adaptive Control Tutorial*. SIAM, 2006.
- [31] Q. Song, F. Liu, J. Cao, and W. Yu, “Pinning-controllability analysis of complex networks: an m-matrix approach,” *Circuits and Systems I: Regular Papers, IEEE Transactions on*, vol. 59, no. 11, pp. 2692–2701, 2012.
- [32] Z. Sun, N. Huang, B. D. Anderson, and Z. Duan, “A new distributed zero-free event-triggered algorithm for multi-agent consensus,” in *Decision and Control (CDC), 2016 IEEE 55th Conference on*, pp. 3444–3449, IEEE, 2016.
- [33] H. Li, X. Liao, T. Huang, and W. Zhu, “Event-triggering sampling based leader-following consensus in second-order multi-agent systems,” *Automatic Control, IEEE Transactions on*, vol. 60, pp. 1998–2003, July 2015.
- [34] W. Hu, L. Liu, and G. Feng, “Consensus of linear multi-agent systems by distributed event-triggered strategy,” *IEEE Transactions on Cybernetics*, vol. 46, pp. 148–157, Jan 2016.
- [35] D. Yang, W. Ren, X. Liu, and W. Chen, “Decentralized event-triggered consensus for linear multi-agent systems under general directed graphs,” *Automatica*, vol. 69, pp. 242–249, 2016.
- [36] B. Wei, F. Xiao, and M.-Z. Dai, “Edge event-triggered control for multi-agent systems under directed communication topologies,” *International Journal of Control*, pp. 1–10, 2017.
- [37] W. Zhu and Z.-P. Jiang, “Event-based leader-following consensus of multi-agent systems with input time delay,” *IEEE Transactions on Automatic Control*, vol. 60, no. 5, pp. 1362–1367, 2015.
- [38] X.-F. Wang, Z. Deng, S. Ma, and X. Du, “Event-triggered design for multi-agent optimal consensus of euler-lagrangian systems,” *Kybernetika*, vol. 53, no. 1, pp. 179–194, 2017.

- [39] J. Mei, W. Ren, and G. Ma, "Distributed Containment Control for Lagrangian Networks With Parametric Uncertainties Under a Directed Graph," *Automatica*, vol. 48, no. 4, pp. 653–659, 2012.
- [40] M. Ye, B. D. O. Anderson, and C. Yu, "Distributed model-independent consensus of Euler–Lagrange agents on directed networks," *International Journal of Robust and Nonlinear Control*, pp. n/a–n/a, 2016. rnc.3689.

APPENDIX A PROOFS FOR SECTION II

A. Lemma 3

Observe that $cxy^2 \leq c\mathcal{X}y^2$ for all $x \in [0, \mathcal{X}]$. It follows that

$$g(x, y) \geq ax^2 + (b - c\mathcal{X})y^2 - dxy$$

if $y \in [0, \infty)$ and $x \in [0, \mathcal{X}]$ because $c > 0$. For any fixed value of $y = y_1 \in [0, \infty)$, write $\bar{g}(x) = ax^2 + (b - c\mathcal{X})y_1^2 - dxy_1$. The discriminant of $\bar{g}(x)$ is negative if

$$b > c\mathcal{X} + \frac{d^2}{4a} \quad (53)$$

which implies that the roots of $\bar{g}(x)$ are complex, i.e. $\bar{g}(x) > 0$ and this holds for any $y_1 \in [0, \infty)$. We thus conclude that for all $y \in [0, \infty)$ and $x \in [0, \mathcal{X}]$, if b satisfies (53), then $g(x, y) > 0$ except the case where $g(x, y) = 0$ if and only if $x = y = 0$.

B. Corollary 1

Observe that $h(x, y) = g(x, y) - ex - fy$ where $g(x, y)$ is defined in **Lemma 3**. Let b^* be such that it satisfies condition (53) in **Lemma 3** and thus $g(x, y) > 0$ for $x \in [0, \infty)$ and $y \in [0, \mathcal{Y}]$. Note that the positivity condition on $g(x, y)$ in **Lemma 3** continues to hold for any $a \geq a^*$ and any $b \geq b^*$. Let a_1 and b_1 be positive scalars whose magnitudes will be determined later. Define $a = a_1 + a^*$ and $b = b_1 + b^*$. Define $z(x, y) \triangleq a_1x^2 + b_1y^2 - ex - fy$. Next, consider $(x, \bar{y}) \in \mathcal{V}$, where \bar{y} is some fixed value. It follows that

$$z(x, \bar{y}) = a_1x^2 - ex + (b_1\bar{y}^2 - f\bar{y})$$

Note the discriminant of $z(x, \bar{y})$ is $\mathcal{D}_x = e^2 - 4a_1(b_1\bar{y}^2 - f\bar{y})$. It follows that $\mathcal{D}_x < 0$ if $b_1\bar{y}^2 > f\bar{y} + e/4a_1$. This is satisfied, independently of $\bar{y} \in [\mathcal{Y} - \varepsilon, \mathcal{Y}]$, for any $b_1 \geq b_{1,y}$, $a_1 \geq a_{1,y}$ where

$$b_{1,y} > \frac{e^2}{4a_{1,y}(\mathcal{Y} - \varepsilon)^2} + \frac{f}{\mathcal{Y} - \varepsilon}$$

because $\mathcal{Y} - \varepsilon \leq \bar{y}$. It follows that $\mathcal{D}_x < 0 \Rightarrow z(x, y) > 0$ in \mathcal{V} . Now, consider $(\bar{x}, y) \in \mathcal{U}$ for some fixed value \bar{x} . It follows that

$$z(\bar{x}, y) = b_1y^2 - fy + (a_1\bar{x}^2 - e\bar{x})$$

and note the discriminant of $z(\bar{x}, y)$ is $\mathcal{D}_y = f^2 - 4b_1(a_1\bar{x}^2 - e\bar{x})$. Suppose that $a_1 > e/\mathcal{X}$, which ensures that $a_1\bar{x}^2 - e\bar{x} > 0$. Then, $\mathcal{D}_y < 0$ if $b_1(a_1\bar{x}^2 - e\bar{x}) > f/4$. This is satisfied, independently of $\bar{x} \in [\mathcal{X} - \vartheta, \mathcal{X}]$, for any $b_1 \geq b_{1,x}$, $a_1 \geq a_{1,x}$ where

$$b_{1,x} > \frac{f}{4(a_{1,x}(\mathcal{X} - \vartheta)^2 - e(\mathcal{X} - \vartheta))}$$

It follows that $\mathcal{D}_y < 0 \Rightarrow z(x, y) > 0$ in \mathcal{U} . We conclude that setting $b = b^* + \max[b_{1,x}, b_{1,y}]$ and $a = a^* + \max[a_{1,x}, a_{1,y}]$, implies $h(x, y) > 0$ in \mathcal{R} , except $h(0, 0) = 0$.

APPENDIX B PROOFS FOR SECTION IV

Before we present the main proof of **Theorem 4**, we need to compute an upper bound using limited information about the initial conditions.

A. An Upper Bound Using Initial Conditions

Suppose that initial conditions are bounded as $\|\mathbf{u}(0)\| \leq k_a$ and $\|\mathbf{v}(0)\| \leq k_b$ with k_a, k_b known a priori. Before we proceed with the main proof, we provide a method to calculate a non-tight upper bound on the initial states expressed as $\|\mathbf{u}(0)\| < \mathcal{X}$ and $\|\mathbf{v}(0)\| < \mathcal{Y}$, with the property that as shown in the sequel, there holds $\|\mathbf{u}(t)\| < \mathcal{X}$ and $\|\mathbf{v}(t)\| < \mathcal{Y}$ for all $t \geq 0$, and exponential convergence results. Due to spatial limitations, we show only the bound on \mathbf{v} and leave the reader to follow an identical process for \mathbf{u} . In keeping with the model-independent nature of the paper, define a function as

$$\bar{V}_\mu = \begin{bmatrix} \mathbf{u} \\ \mathbf{v} \end{bmatrix}^\top \begin{bmatrix} \lambda_{\max}(\mathbf{Q})\mathbf{I}_{np} & \frac{1}{2}\mu^{-1}\bar{\gamma}(k_{\bar{M}} + \delta)\mathbf{I}_{np} \\ \frac{1}{2}\mu^{-1}\bar{\gamma}(k_{\bar{M}} + \delta)\mathbf{I}_{np} & \frac{1}{2}\bar{\gamma}(k_{\bar{M}} + \delta)\mathbf{I}_{np} \end{bmatrix} \begin{bmatrix} \mathbf{u} \\ \mathbf{v} \end{bmatrix} \quad (54)$$

where $\mathbf{Q} = \mathbf{\Gamma}\mathcal{L}_{22} + \mathcal{L}_{22}^\top\mathbf{\Gamma}$, $\underline{\gamma} = \min_i \gamma_i$ and $\bar{\gamma} = \max_i \gamma_i$. Here, γ_i are the diagonal entries of $\mathbf{\Gamma}_p$. The constant $\delta > 0$ is arbitrarily small and fixed. Note that $(k_{\bar{M}} + \delta)\mathbf{I}_{np} > \mathbf{M}$ and that \bar{V}_μ is *not* a Lyapunov function. Let the matrix in (54) be \mathbf{L}_μ . Then according to **Theorem 2**, $\mathbf{L}_\mu > 0$ if and only if $\lambda_{\max}(\mathbf{Q})\mathbf{I}_{np} - \frac{1}{2}\mu^{-2}\bar{\gamma}(k_{\bar{M}} + \delta)\mathbf{I}_{np} > 0$ which is implied by $\lambda_{\max}(\mathbf{Q}) - \frac{1}{2}\mu^{-2}\bar{\gamma}(k_{\bar{M}} + \delta) > 0$. Then $\mathbf{L}_\mu > 0$ for any $\mu \geq \mu_1^*$ where

$$\mu_1^* > \sqrt{\frac{\bar{\gamma}(k_{\bar{M}} + \delta)}{2\lambda_{\max}(\mathbf{Q})}}$$

While \bar{V}_μ is a function of $\mathbf{u}(t)$ and $\mathbf{v}(t)$, we use $\bar{V}_\mu(t)$ to denote $\bar{V}_\mu(\mathbf{u}(t), \mathbf{v}(t))$. Lastly, observe that

$$\begin{aligned} \bar{V}_\mu &\leq \lambda_{\max}(\mathbf{Q})\|\mathbf{u}\|^2 + \frac{1}{2}\bar{\gamma}(k_{\bar{M}} + \delta)\|\mathbf{v}\|^2 \\ &\quad + \mu^{-1}\bar{\gamma}(k_{\bar{M}} + \delta)\|\mathbf{u}\|\|\mathbf{v}\| \end{aligned}$$

Next, let

$$\underline{V}_\mu = \begin{bmatrix} \mathbf{u} \\ \mathbf{v} \end{bmatrix}^\top \begin{bmatrix} \frac{1}{4}\lambda_{\min}(\mathbf{Q})\mathbf{I}_{np} & \frac{1}{2}\mu^{-1}\underline{\gamma}(k_{\underline{M}} - \delta)\mathbf{I}_{np} \\ \frac{1}{2}\mu^{-1}\underline{\gamma}(k_{\underline{M}} - \delta)\mathbf{I}_{np} & \frac{1}{2}\underline{\gamma}(k_{\underline{M}} - \delta)\mathbf{I}_{np} \end{bmatrix} \begin{bmatrix} \mathbf{u} \\ \mathbf{v} \end{bmatrix} \quad (55)$$

Call the matrix in (55) \mathbf{N}_μ . Let the arbitrarily small δ be such that $(k_{\underline{M}} - \delta) > 0$. Analysis using **Theorem 2**, similar to above, is used to conclude that $\mathbf{N}_\mu > 0$ for any $\mu \geq \mu_2^*$ where

$$\mu_2^* > \sqrt{\frac{2\underline{\gamma}(k_{\underline{M}} - \delta)}{\lambda_{\min}(\mathbf{Q})}}$$

Set $\mu_3^* = \max\{\mu_1^*, \mu_2^*\}$. Define

$$\begin{aligned} \rho_1(\mu) &= \frac{1}{2}(k_{\bar{M}} + \delta) - \frac{1}{4}\mu^{-2}(k_{\bar{M}} + \delta)^2\lambda_{\max}(\mathbf{Q})^{-1} \\ \rho_2(\mu) &= \frac{1}{2}(k_{\underline{M}} - \delta) - \mu^{-2}(k_{\underline{M}} - \delta)^2\lambda_{\min}(\mathbf{Q})^{-1} \\ \rho_3(\mu) &= \frac{1}{2}(k_{\underline{M}} - \delta) - \frac{1}{2}\mu^{-2}(k_{\bar{M}})^2\|\mathbf{Q}^{-1}\| \end{aligned}$$

and observe that for sufficiently large μ there holds $\rho_1 \geq \rho_3 > \rho_2$. Assume without loss of generality that $\rho_1 \geq \rho_3 > \rho_2$ (if not, one can always replace μ_3^* by a μ_4^* with $\mu_4^* > \mu_3^*$, and such that $\rho_1 \geq \rho_3 > \rho_2$). Note that for any $\mu \geq \mu_3^*$ there holds $\rho_i(\mu_3^*) \leq \rho_i(\mu)$, $i = 1, 2$. Compute now

$$\bar{V}^* = \lambda_{\max}(\mathbf{Q})k_a^2 + \frac{1}{2}\bar{\gamma}(k_{\bar{M}} + \delta)k_b^2 + \mu_3^{*-1}\bar{\gamma}(k_{\bar{M}} + \delta)k_a k_b$$

One can verify that for any $\mu \geq \mu_3^*$ that $\bar{V}_\mu(0) \leq \bar{V}^*$. It follows from **Lemma 2** and (2b) that

$$\|\mathbf{v}(0)\|_2 \leq \sqrt{\frac{\bar{V}_\mu(0)}{\rho_1(\mu)}} \leq \sqrt{\frac{\bar{V}_\mu(0)}{\rho_1(\mu_3^*)}} < \sqrt{\frac{\bar{V}^*}{\rho_2(\mu_3^*)}} := \mathcal{Y}_1 \quad (56)$$

Follow a similar method to obtain \mathcal{X}_1 . Next, compute

$$\hat{V}^* = \lambda_{\max}(\mathbf{Q})\mathcal{X}_1^2 + \frac{1}{2}\bar{\gamma}(k_{\bar{M}} + \delta)\mathcal{Y}_1^2 + \mu_3^{*-1}\bar{\gamma}(k_{\bar{M}} + \delta)\mathcal{X}_1\mathcal{Y}_1$$

Finally, compute the bound $\mathcal{Y} = \sqrt{\hat{V}^*/\rho_2(\mu_3^*)}$, and note that $\bar{V}_{\mu_3^*} \leq \hat{V}^*$. Note also that $\bar{V}_\mu, \bar{V}^*, \rho_2(\mu_3^*)$ are independent of μ . Thus $\|\mathbf{v}(0)\|_2 < \mathcal{Y}$ (and similarly $\|\mathbf{u}(0)\|_2 < \mathcal{X}$) can be used for all $\mu \geq \mu_3^*$. We now proceed to the proof of **Theorem 4**.

B. Proof of Theorem 4

Part 1: Consider the Lyapunov-like candidate function

$$V = \frac{1}{2}\mathbf{u}^\top \mathbf{Q} \mathbf{u} + \frac{1}{2}\mathbf{v}^\top \Gamma_p \mathbf{M} \mathbf{v} + \mu^{-1}\mathbf{u}^\top \Gamma_p \mathbf{M} \mathbf{v} \quad (57)$$

where $\Gamma_p = \Gamma \otimes \mathbf{I}_p$. It may also be expressed as a quadratic in the variables \mathbf{u} and \mathbf{v}

$$V = \begin{bmatrix} \mathbf{u} \\ \mathbf{v} \end{bmatrix}^\top \begin{bmatrix} \frac{1}{2}\mathbf{Q} & \frac{1}{2}\mu^{-1}\Gamma_p \mathbf{M} \\ \frac{1}{2}\mu^{-1}\Gamma_p \mathbf{M} & \frac{1}{2}\Gamma_p \mathbf{M} \end{bmatrix} \begin{bmatrix} \mathbf{u} \\ \mathbf{v} \end{bmatrix} \quad (58)$$

Theorem 2 is used to conclude that V is positive definite if

$$\frac{1}{2}\mathbf{Q} - \frac{1}{2}\mu^{-2}\Gamma_p \mathbf{M} > 0 \quad (59)$$

which is implied by

$$\lambda_{\min}(\mathbf{Q}) - \mu^{-2}\bar{\gamma}\lambda_{\max}(\mathbf{M}) > 0 \quad (60)$$

Observe that (60) is implied by

$$\mu > \sqrt{\frac{\bar{\gamma}k_{\bar{M}}}{\lambda_{\min}(\mathbf{Q})}} \quad (61)$$

because there holds $\lambda_{\max}(\mathbf{M}) \leq k_{\bar{M}}$. Since $\lambda_{\min}(\mathbf{Q}) > 0$ then there can always be found a $\mu > 0$ which satisfies (61). Define μ_5^* such that μ_5^* satisfies (61) and $\mu_5^* \geq \mu_3^*$. Therefore V is positive definite in \mathbf{u} and \mathbf{v} for all $\mu \geq \mu_5^*$. Denote the matrix in (58) as \mathbf{G} . Following the method outlined in the appendix of [40], it is straightforward to show that $V(t) < \bar{V}_\mu(t)$ for all t because $\mathbf{L}_\mu > \mathbf{G} > \mathbf{N}_\mu$ for all $\mu \geq \mu_5^*$. Lastly, observe that

$$V(t) \leq \frac{1}{2}\lambda_{\max}(\mathbf{Q})\|\mathbf{u}(t)\|^2 + \frac{1}{2}\bar{\gamma}k_{\bar{M}}\|\mathbf{v}(t)\|^2 + \mu^{-1}\bar{\gamma}k_{\bar{M}}\|\mathbf{u}(t)\|\|\mathbf{v}(t)\| \quad (62)$$

Taking the derivative of V with respect to time along the trajectories of the system (36), we have

$$\begin{aligned} \dot{V} &= \mathbf{u}^\top \mathbf{Q} \mathbf{v} + \mathbf{v}^\top \Gamma_p \mathbf{M} \dot{\mathbf{v}} + \frac{1}{2}\mathbf{v}^\top \Gamma_p \dot{\mathbf{M}} \mathbf{v} \\ &\quad + \mu^{-1}\mathbf{v}^\top \Gamma_p \mathbf{M} \mathbf{v} + \mu^{-1}\mathbf{u}^\top \Gamma_p \dot{\mathbf{M}} \mathbf{v} + \mu^{-1}\mathbf{u}^\top \Gamma_p \mathbf{M} \dot{\mathbf{v}} \end{aligned} \quad (63)$$

$$\begin{aligned} &= -\frac{1}{2}\mu\mathbf{v}^\top \mathbf{Q} \mathbf{v} - \frac{1}{2}\mu^{-1}\mathbf{u}^\top \mathbf{Q} \mathbf{u} + \mu^{-1}\mathbf{v}^\top \Gamma_p \mathbf{M} \mathbf{v} \\ &\quad + \mu^{-1}\mathbf{u}^\top \Gamma_p \mathbf{C}^\top \mathbf{v} - \mathbf{v}^\top \Gamma_p \mathbf{e} - \mu^{-1}\mathbf{u}^\top \Gamma_p \mathbf{e} \end{aligned} \quad (64)$$

We obtain (64) by substituting in $\mathbf{M}\dot{\mathbf{v}}$ from (35) noting that $\dot{\mathbf{M}} - 2\mathbf{C}$ is skew-symmetric, or equivalently $\dot{\mathbf{M}} = \mathbf{C} + \mathbf{C}^\top$. Using the properties of the Euler-Lagrange system (P1 to P5), the following upper bound on \dot{V} is obtained.

$$\begin{aligned} \dot{V} &\leq -\left(\frac{1}{2}\mu\lambda_{\min}(\mathbf{Q}) - \mu^{-1}k_{\bar{M}}\bar{\gamma}\right)\|\mathbf{v}\|^2 - \frac{1}{2}\mu^{-1}\lambda_{\min}(\mathbf{Q})\|\mathbf{u}\|^2 \\ &\quad + \mu^{-1}k_C\bar{\gamma}\|\mathbf{v}\|^2\|\mathbf{u}\| + \bar{\gamma}\|\mathbf{v}\|\|\mathbf{e}\| + \mu^{-1}\bar{\gamma}\|\mathbf{u}\|\|\mathbf{e}\| \end{aligned} \quad (65)$$

Using the bound on $\|\mathbf{e}\|$ computed in (34), we then evaluate (65) to be

$$\begin{aligned} \dot{V} &\leq -\left(\frac{1}{2}\mu\lambda_{\min}(\mathbf{Q}) - \mu^{-1}k_{\bar{M}}\bar{\gamma}\right)\|\mathbf{v}\|^2 - \frac{1}{2}\mu^{-1}\lambda_{\min}(\mathbf{Q})\|\mathbf{u}\|^2 \\ &\quad + \mu^{-1}k_C\bar{\gamma}\|\mathbf{v}\|^2\|\mathbf{u}\| + \mu^{-1}\beta_1\bar{\gamma}\|\mathcal{L}_{22}\|\|\mathbf{u}\|\|\mathbf{v}\| \\ &\quad + \beta_2\bar{\gamma}\|\mathcal{L}_{22}\|\|\mathbf{v}\|^2 + \mu^{-2}\beta_1\bar{\gamma}\|\mathcal{L}_{22}\|\|\mathbf{u}\|^2 \\ &\quad + \mu^{-1}\beta_2\bar{\gamma}\|\mathcal{L}_{22}\|\|\mathbf{u}\|\|\mathbf{v}\| + \mu^{-1}\bar{\omega}(t)\bar{\gamma}\|\mathbf{u}\| + \bar{\omega}(t)\bar{\gamma}\|\mathbf{v}\| \end{aligned} \quad (66)$$

$$\begin{aligned} &= -\mu^{-1}\left[A_1\|\mathbf{u}\|^2 + A_2\|\mathbf{v}\|^2 - A_3\|\mathbf{v}\|^2\|\mathbf{u}\| - A_4\|\mathbf{v}\|\|\mathbf{u}\| - A_5\|\mathbf{u}\| - A_6\|\mathbf{v}\|\right] \\ &\quad := -\mu^{-1}p(\|\mathbf{u}\|, \|\mathbf{v}\|) \end{aligned} \quad (67)$$

where $A_1(\mu) = \lambda_{\min}(\mathbf{Q})/2 - \mu^{-1}\bar{\gamma}\beta_1\|\mathcal{L}_{22}\|$, $A_2(\mu) = \mu^2\lambda_{\min}(\mathbf{Q})/2 - \bar{\gamma}(k_{\bar{M}} + \mu\beta_2)$, $A_3 = k_C\bar{\gamma}$, $A_4 = \|\Gamma\mathcal{L}_{22}\|\bar{\gamma}(\beta_1 + \beta_2)$, $A_5(t) = \bar{\gamma}\bar{\omega}(t)$, and $A_6(\mu, t) = \mu\bar{\gamma}\bar{\omega}(t)$. By designing β_1 such that

$$\beta_1 < \frac{\mu_5^*\lambda_{\min}(\mathbf{Q})}{2\bar{\gamma}\|\mathcal{L}_{22}\|}$$

then $A_1(\mu) > 0$ for any $\mu \geq \mu_5^*$. Observe that $A_2(\mu_5^*) > 0$ if $(\mu_5^*)^2\lambda_{\min}(\mathbf{Q})/2 - \bar{\gamma}k_{\bar{M}} - \mu_5^*\beta_2 > 0$. Rearranging for β_2 , this is implied by

$$\beta_2 < \frac{\mu_5^*\lambda_{\min}(\mathbf{Q})}{2} - \frac{\bar{\gamma}k_{\bar{M}}}{\mu_5^*} \quad (68)$$

and note that any β_2 satisfying (68) continues to satisfy (68) for any $\mu \geq \mu_5^*$. If the right hand side of (68) is negative, it is still possible to ensure that $A_2(\mu_5^*) > 0$ by increasing the size of μ_5^* and setting β_2 sufficiently small because the coefficient of μ^2 in A_2 is positive. Lastly, observe that as $\mu \rightarrow \infty$ then $A_1(\mu) \rightarrow \lambda_{\min}(\mathbf{Q})/2$, $A_2(\mu) = \mathcal{O}(\mu^2)$ and $A_6(\mu) = \mathcal{O}(\mu)$. Notice that $\bar{\omega}(t)$ decays to 0 exponentially fast. In other words, the coefficients $A_5(t)$ and $A_6(\mu, t)$ decay to zero exponentially fast.

Part 2: We now show that the trajectories of the system are bounded for all time by carefully designing μ . For *Part 2* and *Part 3* of the proof, a diagram is included in Fig. 10 to aid in

the explanation of the proof. Notice that $p(\|\mathbf{u}\|, \|\mathbf{v}\|)$ in (67) is of the same form as $h(x, y)$ in **Corollary 1** with $\|\mathbf{u}\| = x$, $\|\mathbf{v}\| = y$ and $A_1(\mu) = a$, $A_2(\mu) = b$, $A_3 = c$, $A_4 = d$, $A_5(0) = e$ and $A_6(\mu, 0) = f$. Note that $A_5(t_1) > A_5(t_2)$ and $A_6(\mu, t_1) > A_6(\mu, t_2)$ for any $t_1 < t_2$. Because of this, we proceed using $A_5(0), A_6(\mu, 0)$: any $A_2(\mu)$ satisfying the inequalities on b in **Corollary 1** for $t = 0$ will continue to satisfy the inequalities for $t > 0$. This will be clear in the sequel. We now use the values \mathcal{X}, \mathcal{Y} computed in subsection B-A. Choose $\vartheta_0 > \mathcal{X} - \mathcal{X}_1$ and $\varphi_0 > \mathcal{Y} - \mathcal{Y}_1$, and ensure that $\mathcal{X} - \vartheta_0, \mathcal{Y} - \varphi_0 > 0$. Note the fact that $\mathcal{X} \geq \mathcal{X}_1$ and $\mathcal{Y} \geq \mathcal{Y}_1$ implies $\vartheta_0, \varphi_0 > 0$. We assume without loss of generality that \mathcal{X} found in Section B-A is such that $\mathcal{X} - \vartheta_0 > A_5(0)/A_1(\mu)$. If this inequality were not satisfied, one would replace \mathcal{X} by a $\bar{\mathcal{X}} > \mathcal{X}$ such that $\bar{\mathcal{X}} - \vartheta_0 > e/a$ and proceed with the stability proof using $\bar{\mathcal{X}}$.

Define the sets \mathcal{U}, \mathcal{V} and the region \mathcal{R} as in **Corollary 1** with $\|\mathbf{u}\| = x$, $\|\mathbf{v}\| = y$. Define further the sets $\bar{\mathcal{U}} = \{\|\mathbf{u}\| : \|\mathbf{u}\| > \mathcal{X}\}$ and $\bar{\mathcal{V}} = \{\|\mathbf{v}\| : \|\mathbf{v}\| > \mathcal{X}\}$. Define the compact region $\mathcal{S} = \mathcal{U} \cup \mathcal{V} \setminus \bar{\mathcal{U}} \cup \bar{\mathcal{V}}$ (refer to Fig. 10 for details). Since $\mathcal{S} \subset \mathcal{R}$, there exists a $\mu_6^* \geq \mu_5^*$ such that $A_2(\mu_6^*)$ satisfies the requirement on b in **Corollary 1**, which ensures that $p(\|\mathbf{u}\|, \|\mathbf{v}\|) > 0$. This in turn implies that $\dot{V} < 0$ in \mathcal{S} . Lastly, define the region $\|\mathbf{u}(t)\| \in [0, \mathcal{X} - \vartheta_0)$ and $\|\mathbf{v}(t)\| \in [0, \mathcal{Y} - \varphi_0)$ as \mathcal{T} . In this part of the proof, we are trying to show that the trajectories of (36) remain bounded for all time. For purposes of explanation, we therefore temporarily assume that \mathcal{S} and \mathcal{T} are time-invariant, as opposed to Fig. 10. In the latter *Part 3*, we will discuss the time-varying nature of $\mathcal{S}(t)$ and $\mathcal{T}(t)$ and show that the boundedness arguments developed here continue to hold.

We are now ready to show that the trajectory of the system (36) remains in $\mathcal{T} \cup \mathcal{S}$ for all $t \geq 0$. We define T_1 as the infimum of time values for which either $\|\mathbf{u}(t)\| < \mathcal{X}$ or $\|\mathbf{v}(t)\| < \mathcal{Y}$ fail to hold. We show that the existence of T_1 creates a contradiction, and thus conclude that the bounds $\|\mathbf{u}(t)\| < \mathcal{X}$ or $\|\mathbf{v}(t)\| < \mathcal{Y}$ hold for all t .

Observe that \dot{V} may be sign indefinite in \mathcal{T} , which means if the trajectory of the system is in \mathcal{T} (the blue region in Fig. 10) then $V(t)$ can increase. However, from (62) we obtain that in \mathcal{T}

$$V(t) \leq \frac{1}{2} \lambda_{\max}(\mathbf{Q})(\mathcal{X} - \vartheta_0)^2 + \frac{1}{2} \bar{\gamma}(k_{\bar{M}} + \delta)(\mathcal{Y} - \varphi_0)^2 + \mu^{-1} \bar{\gamma}(k_{\bar{M}} + \delta)(\mathcal{X} - \vartheta_0)(\mathcal{Y} - \varphi_0) := \mathcal{Z}$$

One can easily verify that $\mathcal{Z} < \hat{V}^*$ because we selected ϑ_0, φ_0 such that $\mathcal{X}_1 > \mathcal{X} - \vartheta_0$ and $\mathcal{Y}_1 > \mathcal{Y} - \varphi_0$. Note that any trajectory of (36) beginning¹ in $\mathcal{S} \cup \mathcal{T}$ must satisfy $V(t) \leq \max\{\mathcal{Z}, V(0)\} < \hat{V}^*$ for $t \in [0, T_1]$. This is because $\dot{V} < 0$ in \mathcal{S} ; any trajectory starting in \mathcal{S} (respectively \mathcal{T}) has $V(t) < V(0)$ (respectively $V(t) < \mathcal{Z}$). If the trajectory leaves \mathcal{T} and enters \mathcal{S} at some t , consider the crossover point, which is in the closure of \mathcal{T} . By the virtue that V is continuous, we have $V(t) < \mathcal{Z}$ and by virtue of entering \mathcal{S} , $V(t + \delta) \leq V(t) < \mathcal{Z}$, for some arbitrarily small δ . Define $\zeta = \lambda_{\min}(\mathbf{M} -$

¹ The definitions of \mathcal{S} and \mathcal{T} ensure that $\mathbf{u}(0), \mathbf{v}(0) \in \mathcal{S} \cup \mathcal{T}$ as evident in (56).

$\mu^{-1} \mathbf{M} \mathbf{Q}^{-1} \mathbf{M})/2$ and verify that $\zeta \geq \rho_3(\mu_3^*) > \rho_2(\mu_3^*)$. In accordance with **Lemma 2** we have

$$\|\mathbf{v}(T_1)\|_2 \leq \sqrt{\frac{V(T_1)}{\zeta}} < \sqrt{\frac{\hat{V}^*}{\zeta}} < \sqrt{\frac{\hat{V}^*}{\rho_2(\mu_3^*)}} = \mathcal{Y} \quad (69)$$

Paralleling the argument leading to (69), one can also show that $\|\mathbf{u}(T_1)\| < \mathcal{X}$. We omit this due to spatial limitations and similarity of argument. The existence of (69) and a similar inequality for $\|\mathbf{u}(T_1)\|$ contradict the definition of T_1 . In other words, T_1 does not exist, and therefore $\|\mathbf{u}(t)\| < \mathcal{X}$ and $\|\mathbf{v}(t)\| < \mathcal{Y}$ for all t , as depicted in Fig 10.

Part 3: We now show that the leader-follower consensus objective is achieved. In order to do this, we firstly explore how the time-varying nature of $A_5(t)$ and $A_6(\mu, t)$ affects \dot{V} . As discussed in Fig. 10, $A_5(t)$ and $A_6(\mu, t)$ decay to zero exponentially fast due to the presence of $\bar{\omega}(t)$. Therefore, at $t = \infty$, $p(\|\mathbf{u}\|, \|\mathbf{v}\|)$ is of the form of $g(x, y)$ in **Lemma 3** and is thus positive definite (and therefore $\dot{V} = -\mu^{-1} p$ is negative definite) for $\|\mathbf{u}\| \in [0, \mathcal{X}]$ and $\|\mathbf{v}\| \in [0, \infty)$. This is because μ_6^* as designed according to **Corollary 1** also satisfies the requirements detailed in **Lemma 3**. It is also straightforward to conclude that the sign indefiniteness of $\dot{V}(t)$ in $\mathcal{T}(t)$ arises due to the terms linear in $\|\mathbf{u}\|$ and $\|\mathbf{v}\|$ in (66), i.e. the terms containing $\bar{\omega}(t)$, which are precisely the coefficients $A_5(t)$ and $A_6(\mu, t)$ in (67).

Now that we have established that $A_5(t)\|\mathbf{u}\|$ and $A_6(\mu, t)\|\mathbf{v}\|$ give rise to the region $\mathcal{T}(t)$, we now establish the precise behaviour of $\mathcal{T}(t)$ and $\mathcal{S}(t)$ as functions of time. Now examine the inequalities on the coefficient b as detailed in **Corollary 1**, applied to $p(\|\mathbf{u}\|, \|\mathbf{v}\|)$ in (67). We conclude that for a fixed μ_6^* , the strictly monotonically decreasing nature of A_5, A_6 then implies that, for fixed $A_2(\mu_6^*)$, the region in which $p(\|\mathbf{u}\|, \|\mathbf{v}\|) > 0$ (respectively sign indefinite) as defined by $\mathcal{S}(t)$ (respectively $\mathcal{T}(t)$), is time-varying. *Specifically, $\vartheta(t)$ and $\varphi(t)$ are strictly monotonically increasing.* Moreover, because $A_5 = A_6 = 0$ at $t = \infty$, we conclude that $\lim_{t \rightarrow \infty} \vartheta(t) = \mathcal{X}$ and $\lim_{t \rightarrow \infty} \varphi(t) = \mathcal{Y}$, at which point $\mathcal{T}(t) = [0, 0]$.

It is straightforward to show that appropriate functions are given by $\vartheta(t) = -a_1 e^{-a_2 t} + \mathcal{X}$ and $\varphi(t) = -b_1 e^{-b_2 t} + \mathcal{Y}$. Here, a_1, a_2, b_1, b_2 are positive constants associated with $\mathcal{X}_0, \mathcal{Y}_0$ and the decay rate of $\bar{\omega}(t)$. Moreover, because $\vartheta(t), \varphi(t)$ are strictly monotonically increasing, it is easy to verify that $\mathcal{S}(t_1) \subset \mathcal{S}(t_2)$ and $\mathcal{T}(t_1) \supset \mathcal{T}(t_2)$ for any $t_1 < t_2$. These properties ensure that the boundedness arguments developed in *Part 2* remain valid for time-varying $\mathcal{S}(t)$ and $\mathcal{T}(t)$ due to the nature of the time variation.

Now that we have established the behaviour of $\mathcal{S}(t)$ and $\mathcal{T}(t)$, we move on to show that leader-follower consensus is achieved. Suppose that at some T_2 , the trajectory of the system (36) leaves $\mathcal{T}(t)$ and does not enter $\mathcal{T}(t)$ for all $t \geq T_2$. In other words, for $t \geq T_2$, the trajectory is in $\mathcal{S}(t)$ (recall that in *Part 2* we established that $\|\mathbf{u}(t)\| < \mathcal{X}$ and $\|\mathbf{v}(t)\| < \mathcal{Y}$ for all t). This is illustrated in Fig. 10.

Firstly, consider the case where $T_2 = \infty$. From the form of $\vartheta(t), \varphi(t)$, we conclude that $\mathcal{T}(t)$ shrinks exponentially fast towards the origin $\mathbf{u} = \mathbf{v} = 0$. If $T_2 = \infty$ then there is some $T_3 < \infty$ such that the trajectory of the system (36) is in $\mathcal{T}(t)$ for all $t \in [T_3, \infty)$. From the limiting behaviour of $\mathcal{T}(t)$,

we conclude that the trajectory of (36) also converges to the equilibrium $\|\mathbf{u}\| = \|\mathbf{v}\| = 0$, which implies that the leader-follower consensus objective has been achieved. Moreover, the convergence rate is exponential for $t \in [T_3, \infty)$.

Secondly, consider the case where T_2 is finite. Note that T_2 is initial condition dependent, but the initial condition set is bounded according to Assumption 3. It follows that there exists a \bar{T}_2 independent of initial conditions such that, for every initial condition satisfying Assumption 3, $T_2 < \bar{T}_2 < \infty$. Define the time interval $t_p = [\bar{T}_2, \infty)$. Because the trajectory of the system (36) is in $\mathcal{S}(t)$ for all $t \in t_p$ then $\dot{V}(t) < 0$ for all $t \in t_p$. Consider some arbitrary time $t_1 \in t_p$. We observe that $p(\|\mathbf{u}\|, \|\mathbf{v}\|) > 0$ (i.e. positive definite) in the compact region $\mathcal{S}(t_1)$. One can therefore find a scalar $a_{1,t_1} > 0$ such that $p(\|\mathbf{u}\|, \|\mathbf{v}\|) \geq a_{1,t_1} \|[\mathbf{u}^\top, \mathbf{v}^\top]^\top\|$ for all $\|\mathbf{u}\|, \|\mathbf{v}\| \in \mathcal{S}(t_1)$. Furthermore, by recalling that A_5, A_6 are positive and strictly monotonically decreasing, we conclude that $p(\|\mathbf{u}\|, \|\mathbf{v}\|, t_1) < p(\|\mathbf{u}\|, \|\mathbf{v}\|, t_2)$ for any \mathbf{u}, \mathbf{v} , and for any $t_1 \leq t_2$ where $t_1, t_2 \in t_p$. It follows that there exists some constant $\bar{a}_1 > 0$ such that $p(\|\mathbf{u}\|, \|\mathbf{v}\|) \geq \bar{a}_1 \|[\mathbf{u}^\top, \mathbf{v}^\top]^\top\|$ for all \mathbf{v}, \mathbf{u} in $\mathcal{S}(t)$, for all $t \in t_p$. This implies that, in $\mathcal{S}(t)$ we have $\dot{V} \leq -\bar{a}_1 \|[\mathbf{u}^\top, \mathbf{v}^\top]^\top\| < 0$ for all $t \in t_p$. The eigenvalues of the constant matrices \mathbf{L}_μ and \mathbf{N}_μ (the matrices introduced in subsection B-A) are finite and strictly positive. Our earlier conclusion that $\mathbf{L}_\mu > \mathbf{G} > \mathbf{N}_\mu$ for all $\mu \geq \mu_3^*$ then implies that the eigenvalues of \mathbf{G} (which vary with $\mathbf{q}(t)$) are upper bounded away from infinity and lower bounded away from zero. It follows that there exist scalars $a_2, a_3 > 0$ such that $a_2 \|[\mathbf{u}^\top, \mathbf{v}^\top]^\top\| \leq V(t) \leq a_3 \|[\mathbf{u}^\top, \mathbf{v}^\top]^\top\|$. This implies that $\dot{V}(t) \leq -\psi V(t)$ in $\mathcal{S}(t)$ for $t \in t_p$ where $\psi = \bar{a}_1/a_3$. From this, we conclude that V decays exponentially fast to zero, with a minimum rate $e^{-\psi t}$, for $t \in t_p$. Since V is positive definite in \mathbf{u}, \mathbf{v} , this implies that $\|[\mathbf{u}^\top, \mathbf{v}^\top]^\top\|$ decays to zero exponentially fast for $t \in t_p$, and the leader-follower consensus objective is achieved.

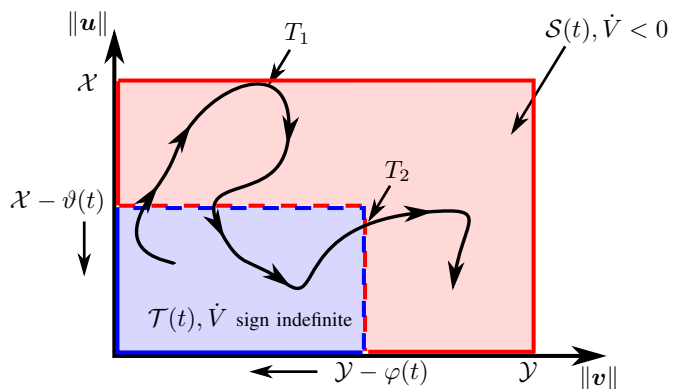


Fig. 10. Diagram for proof of **Theorem 4**. The red region is $\mathcal{S}(t)$, in which $\dot{V}(t) < 0$ for all $t \geq 0$. The blue region is $\mathcal{T}(t)$, in which $\dot{V}(t)$ is sign indefinite. A trajectory of (36) is shown with the black curve. At $t = T_1$, it is shown in *Part 2* that the trajectory of (36) is such that $\|\mathbf{u}(T_1)\| < \mathcal{X}$, $\|\mathbf{v}(T_1)\| < \mathcal{Y}$ and thus the trajectory does not leave $\mathcal{S}(t)$. The sign indefiniteness of $\dot{V}(t)$ in $\mathcal{T}(t)$ arises due to the terms linear in $\|\mathbf{u}\|$ and $\|\mathbf{v}\|$ in (66), i.e. the terms containing $\bar{\omega}(t)$ (coefficients $A_5(t)$ and $A_6(\mu, t)$ in (67)). Because $\bar{\omega}(t)$ goes to zero at an exponential rate, so do the coefficients $A_5(t)$ and $A_6(\mu, t)$. Examining the inequalities detailed in **Corollary 1** as applied to $p(\|\mathbf{u}\|, \|\mathbf{v}\|)$ in (67), it is straightforward to conclude that for a fixed μ_6^* , the exponential decay of A_5, A_6 implies that the region $\mathcal{T}(t)$ shrinks towards the origin at an exponential rate. In other words, $\vartheta(t)$ and $\varphi(t)$ monotonically increase until $\vartheta(t) = \mathcal{X}$ and $\varphi(t) = \mathcal{Y}$, at which point $\mathcal{T}(t) = [0, 0]$. This corresponds to the dotted red and blue lines, which show, respectively, the time-varying boundaries of $\mathcal{S}(t)$ and $\mathcal{T}(t)$. The solid red and blue lines show respectively, the boundaries of $\mathcal{S}(t)$ and $\mathcal{T}(t)$, which are time-invariant. Exponential convergence to the leader-follower objective is discussed in *Part 3* making use of T_2 .